1993

A probabilistic analysis for transmission line structures

Kristine Marie Sandage
Iowa State University

A probabilistic analysis for transmission line structures

by

Kristine Marie Sandage

A Thesis Submitted to the
Graduate Faculty in Partial Fulfillment of the
Requirements for the Degree of
MASTER OF SCIENCE

Department: Civil and Construction Engineering
Major: Civil Engineering (Structural Engineering)

Approved:
Signatures redacted for privacy.

Iowa State University
Ames, Iowa

1993

TABLE OF CONTENTS

LIST OF FIGURES

LIST OF TABLES

1. INTRODUCTION

Probabilistic methods and procedures are becoming more common in the analysis and design of structural members, and are especially useful when evaluating failed structures such as transmission line structures. These techniques allow the designer to account for the uncertainty associated with material and geometric parameters such as structure height, cross-sectional area of the pole, thickness of the pole, distance between bracing, and material yield strength.

1.1 History of Recent Failures

Recently in Mid-Iowa transmission lines failed twice because of severe ice storms which involved H-frame hollow tubular steel structures. The first ice storm occurred in early spring of 1990, when a portion of the Lehigh-Sycamore 345-kv electric transmission line was damaged, resulting in structural failures of 68 transmission structures [1]. Figure 1.1 shows the damaged portion of the line and its location.

On March 7, 1990, the southwest and central parts of Iowa experienced a severe ice storm that caused large amounts of ice to accumulate on the conductors. The amount of ice on the conductors recorded on the following morning, 14 hours later and at 40 degrees F, was approximately 1.25 to 1.5 in. [1].

Static, dynamic and buckling analyses using a three-dimensional, finite element computer model were performed to

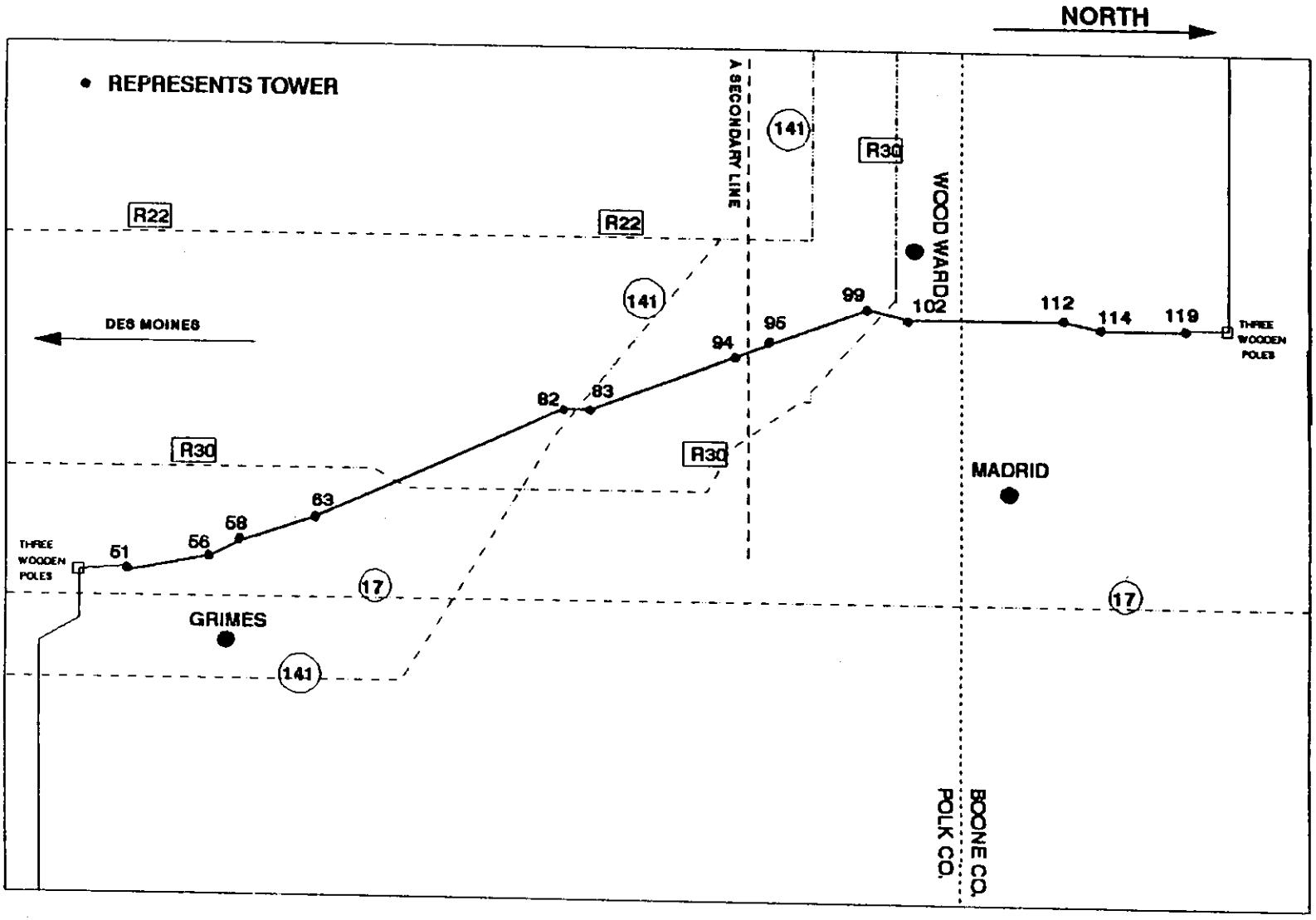

Fig. 1.1: Damaged portion of the Lehigh-Sycamore transmission line and its location.

determine possible failure scenarios and the line failure load [1]. The finite element analysis included both geometric and material nonlinear behavior of the system and was executed on the Electric Power Research Institute's TLWorkstation (module ETADS) finite element analysis software [2]. However, these analyses were conducted based on the assumption that the material and geometric parameters were deterministic quantities; not accounting for any variabilities that exist in the actual structure.

Structural analysis revealed that the transmission line failure could have initiated somewhere between 1.5 to 1.75 in. of ice load. On the basis of the analysis results, field observations, and hypothesis, two possible failure scenarios leading to the collapse of the transmission line were established.

In the first scenario, the study suggested that initial failure of one of the insulators (or its hardware components or both the insulator and the hardware components) resulted in the separation of the conductor from the tower. Consequently, this occurrence caused the loss of the line tension in the conductor which finally led to the buckling in a domino pattern of the structures from unbalanced longitudinal forces.

In the second scenario, initial buckling of one of the structures was caused by galloping conductor forces at 1.5 in. of ice. Galloping of a conductor is a phenomenon usually

caused by a relatively strong wind blowing on an iced conductor [1]. This second scenario was deemed to be less likely because of the field observations and analytical results.

The first failure scenario was verified analytically and was consistent with evidence from field observations.

The second ice storm occurred only 18 months later beginning on October, 31, 1991, on a different segment of the same electric transmission line in which over 30 miles of structures collapsed because of the storm [3]. The weather conditions resulted in more ice accumulation than the March 7, 1990 storm and was the most destructive ice storm in Iowa history [4]. Investigation is in progress to predict, if possible, the cause of the failure [3].

As a result of the previous work, the recommendation made in Ref. 1 was that "a probabilistic analysis needs to be developed that can take into account uncertainty associated with design parameters such as material and geometrical imperfections and variability in the loading." Incorporating the randomness associated with the material and geometric parameters as well as the variability in the ice thickness allows a more realistic representation of the performance of the transmission line structure to be achieved.

1.2 Objectives

The objective of this work was to develop a procedure to determine the strength of a transmission line structure under ice loading by using a probabilistic method. The strength of a transmission structure is defined herein by the load which:

- causes elastic instability of the structure
- produces forces in a component beyond its capacity
- results in formation of a mechanism resulting in a large rotation.

The evaluated strength can then be used to develop a fragility curve relating the probability of failure to a given ice thickness on the conductor (see Fig. 1.2).

The focus of this work was to accomplish three primary objectives:

1. To outline the basic analysis procedure.
2. To validate the basic analysis procedure utilizing published information.
3. To demonstrate the procedure on an actual transmission line structure.

1.3 Organization of the Study

A literature study was performed to review relevant reliability studies. In addition, the statistics and the reliability theories used by other research or in investigating the performance of the structures was reviewed.

Next, the basic analysis procedure for the probabilistic analysis of transmission line structures was developed. This followed the reliability strategies given in Ref. 5, 6, 7, 8.

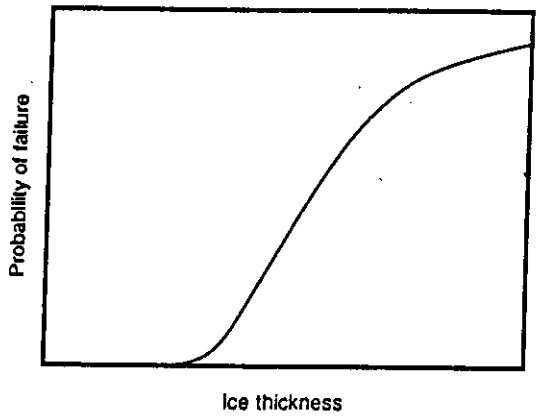

Fig. 1.2: Typical fragility curve.

The method was validated by using simple truss and portal frame examples.

Lastly, the procedure was applied to an actual transmission structure from the second line failure described in Ref. 3. To demonstrate the procedure, the structural analysis utilized the ETADS software developed by the Electric Power Research Institute (EPRI). This program is a structural finite element routine designed for specific application to transmission line structures [2]. The software is capable of incorporating large displacements and material nonlinearity in formulating the structural stiffness matrix. Also, a statistical analysis program (SAS) [9] was employed for the statistical calculations in conjunction with various developed spreadsheets for reliability computations.

2. LITERATURE REVIEW AND BACKGROUND

Transmission line structures play a vital role in the function of providing electricity to practically every household, business and organization. These structures are subjected to many kinds of climatic conditions. In fact, the probability is very high that a structure will be under extreme stress from exposure to such conditions as ice accumulation on the conductors and high winds. Therefore, the design objective is to proportion a reliable structure which will remain in service and will not require excessive maintenance after every storm. Research has been conducted in the areas of transmission line structural loads, design methodologies and reliability concepts. In the following sections, past research conducted in each of these areas is briefly discussed.

2.1 Transmission Line Structural Loading

In the past, the National Electric Safety Code (NESC) [10] has been the primary source in the United States for selecting the minimal design loads of transmission line structural design. Design loads include dead, climate, accident, construction and maintenance loads. The NESC uses combinations of loading conditions on the line to calculate structural loads which are multiplied by overload factors (load factors) to achieve structural safety [10].

Probabilistic methods and procedures are becoming more common design tools for steel, concrete and transmission line structures. For example, several design techniques for transmission lines have been proposed in the past few years to utilize probability based climatic loads. Two of these reliability based design methods for transmission lines, which will be discussed in more detail in the next section, have received the most attention and are now available to design engineers for trial use [11]. The American Society of Civil Engineers (ASCE) [12] and International Electrotechnical Commission (IEC) [13] have proposed procedures which are quite different in the calculation of the load caused by a climatic event. The most significant difference between the two techniques concerns the availability of weather data specified by each document. The ASCE method uses data that are generally available; whereas, the IEC method utilizes data that are yet not commonly available, such as extreme wind or ice in the region of the line, ice weight per unit length and ice shape [11]. The IEC procedure requires the analyst to consider several more load combinations than the number specified in the ASCE method [11].

2.2 Design Methodologies

As stated above, the NESC has typically been the primary source for the minimal design of transmission line structures. However, with the advent of reliability based design

procedures of transmission line structures, the NESC may be replaced or updated by procedures incorporating these newer probabilistic methods [14].

Continuing the comparison of the ASCE and IEC methods of reliability design, the ASCE method utilizes procedures for sizing different structural components based on predefined target reliability levels. On the other hand, the IEC technique focuses on a system-based concept and does not provide specific guidance for the design of the individual components. According to Ref. 11, the ASCE method is easier and more straight forward to implement than the IEC procedure.

The IEC and ASCE definition of system is another key difference between the two concepts. When ASCE uses the term system, the reference is to one transmission line structure. Hence, when ASCE refers to system reliability, the reference is only to the reliability of a single transmission structure. However, the IEC definition of the system refers to the entire transmission line. Therefore, the term system reliability refers to the transmission line including all the structures supporting the line.

Using the IEC definition of system, system reliability concepts in the design of transmission line structures may include hundreds of miles and must consider several loading combinations. Among these cases are the wind and ice loadings. Unfortunately, no reliable statistics describing

the variation in these loads would be known prior to the occurrence of a failure event. This causes difficulties and uncertainties in the calculation of reliability of the line being investigated.

2.3 Reliability Background

The following summarizes the basic reliability principals, calculations of failure probabilities, as well as some of the previously published techniques to analyze transmission line structures using probabilistic methods.

2.3.1 Limit state functions

Reliability of a system is defined as the probability that the system is safe to withstand an applied load or loads. However, the probability of failure for a system has been more common in describing the performance of a structure. Determination of the probability of failure begins with definition of the limit state functions of the system.

The limit state function is described as the conditions beyond which the system cannot perform the function for which it was designed. These conditions can either pertain to safety or performance depending on the limit state under consideration. In other words, a limit state represents only one failure mode of the system, and sometimes several limit states can be involved in the calculation of the probability of failure for one system.

For the specific case of the transmission line structure, the structure is designed for the function of supporting the conductors, which are attached to the structure by an insulator assembly. For clarification, the insulator assembly is shown in Fig. 2.1.

Some examples are listed below of the transmission structure failure modes where it fails to serve its purpose in supporting the conductors:

- elastic instability of the structure
- forces in a component beyond its capacity
- formation of a mechanism resulting in a large rotation that results in a collapse of the transmission structure.

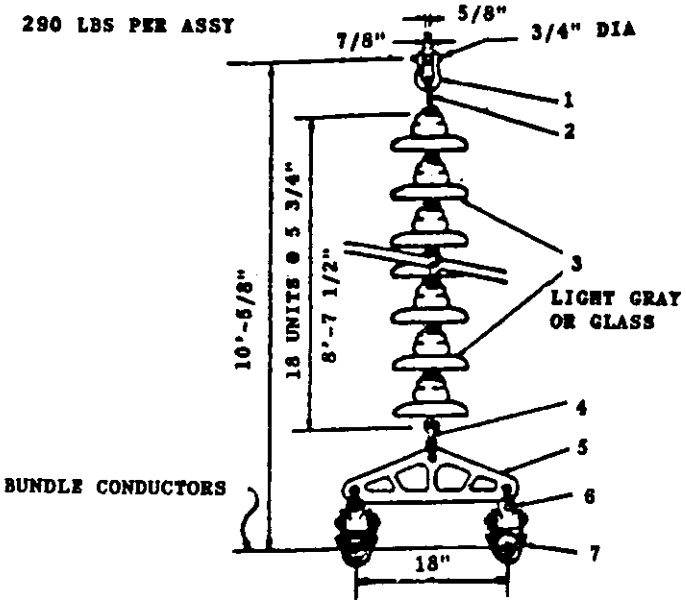

ITEM	QTY	DESCRIPTION
1	1	ANCHOR SHACKLE
2	1	OVAL EYE BALL
3	18	INSULATOR UNITS
4	1	SOCKET "Y" CLEVIS
5	2	EYE "Y" CLEVIS
6	2	SUSPENSION CLAMP
7	1	YOKE PLATE

Fig. 2.1: A typical insulator assembly.

Each type of failure listed above constitutes a different limit state.

The limit state function, G, is based on the difference between the random structural resistance variable, R, and the load variable, Q, which is numerically shown as:

$$G = R\{x_i\} - Q \qquad (2.1)$$

where x_i represent the geometric and material parameters that are used to evaluate the resistance, R. More details concerning the procedure used in this work will be discussed in the next chapter.

2.3.2 Levels of analysis

Once the limit states are stated in terms of the variables, x_i, the calculation of the probability of failure is accomplished on one of three levels. Each level has a progressively higher level of sophistication with respect to the analysis procedure. In the following, discussion will progress from the highest level (level 3) to the lowest level (level 1). The highest level is the most complete and accurate representation of the computation of the probability of failure.

2.3.2.1 Level 3: reliability analysis

At level 3, the probability of failure is measured by a multidimensional integration of the joint probabilities of the resistance and load. Letting $f_R(r)$ characterize the density

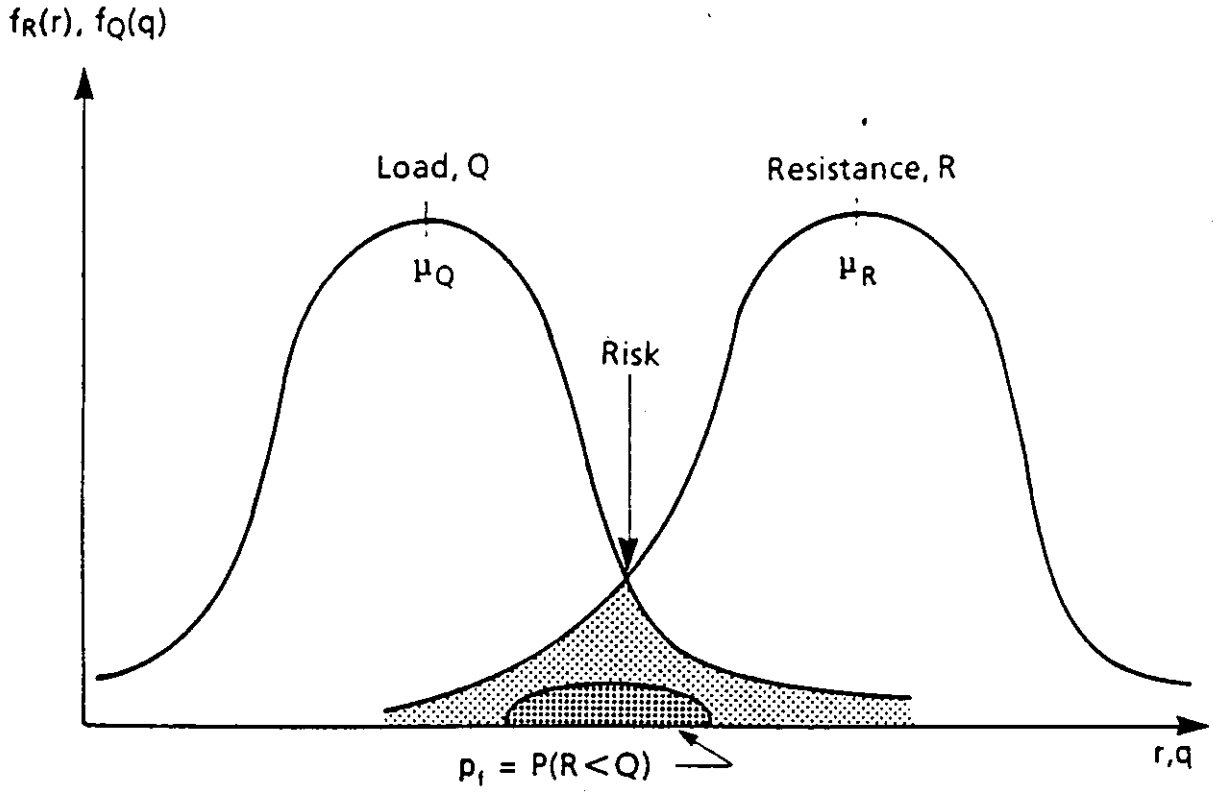

Fig. 2.2: Fundamental reliability problem.

function of the resistance, and $f_Q(q)$ denote that density function of the load, the integration of the following equation results in the exact probability of failure:

$$p_f = P(R \leq Q) = \int_{-\infty}^{\infty} f_Q(q) \int_{-\infty}^{q} f_R(r)\, dr dq \qquad (2.2)$$

The graphical representation of the probability distributions of the resistance and the load is shown in Fig. 2.2, with the

area portraying the probability of failure, p_f, also being indicated.

This computation requires full knowledge of the distribution functions and is extremely difficult to evaluate; the complexity of this computation even renders many cases impossible to evaluate. For this reason, Monte Carlo simulation methods are more common. These methods simulate finite values of the resistance and load to find the probability of failure utilizing computer analysis. However, this approach requires a large number of runs (3000 to 4000, according to Ref. 16) to produce a statistically reliable probability of failure, which may be very time consuming.

2.3.2.2 Level 2: reliability analysis

Due to the deficiencies of level 3, level 2 methods make assumptions and simplifications in order to make the calculation of the probability of failure easier. The sacrifice of making these simplifications results in an approximate value for the probability of failure. The essence of level 2 methods entail checking a finite number of points (usually only one point at the mean values of the variables) on the limit state function surface. For comparison, level 3 involves checking of all points along the entire surface of the limit state function.

2.3.2.3 Level 1: reliability analysis

Level 1 entails the most simplistic approach of all three. This approach encompasses design and safety checking methods, because only a single characteristic value is connected to each variable. In actuality, no probability of failure calculations are performed; so level 1 methods are not really methods of reliability analysis [8]. However, level 1 operational methods provide engineers with a basis for design code provisions.

Level 2 balances the disadvantages and benefits involved in the calculation of the probability of failure better than the other levels; accordingly, it is the focus of this research. Within level 2, the particular method that will be applied to this work is the First Order-Second Moment (FOSM) method.

2.3.3 Reliability analyses of transmission line structures

Due to the different reliability levels of analysis and various methods available within each level, numerous reliability methods have been applied to the analyses of transmission line structures. Details of some of these methods will be discussed in this section.

2.3.3.1 Reliability relationship between line and structure

The system reliability may refer to the entire transmission line encompassing miles of transmission

structures, or to a single transmission line structure. In the first case, the reliability analysis must not only consider the variation of the load processes that affect the line, but also the spatial correlations within and among these load processes.

A method for relating the reliability of these two aspects of system, (the transmission line and the transmission structure), has been developed by Dagher, Kulendran, Peyrot, and Maamouri [15]. This method calculates the probability of failure of a line segment, PF_L, as

$$PF_L = \alpha \ (N/n) \ PF_S \qquad (2.3)$$

where,

PF_S= probability of failure of a structure,
α = system reliability usage factor,
N= total number of structures in line segment, and
n= number of structures simultaneously subjected to the same extreme climatic event.

This relationship accounts for the spatial extent of the extreme loading events within the system reliability usage factor, α. The factor, α, is obtained in this source by using Monte Carlo simulation for extreme wind and extreme ice loadings.

This analysis was able to use available weather data to estimate the probability of failure of the line by converting the problem from an event-based formulation to an extreme value analysis.

2.3.3.2 Monte Carlo example

Level 2 techniques are most frequently implemented, but level 3 is often employed when Monte Carlo simulations are needed to validate level 2 methods.

A censoring technique for Monte Carlo simulations was proposed by Kamarudin [16] that reduced the number of simulations, and thus reduced the cost and time involved in analysis. The benefit of the censoring technique is the ability to determine if individual trials are failures or survivals without going through the structural calculations. The amount of savings involved with this procedure is variable, but may be as much as a 30% reduction of the amount of computations. Kamarudin tested this technique on a wood pole design.

This technique involved checking the resistance of the structure during each trial and deciding if further structural calculations were required. If the resistance satisfied a predetermined check-point criteria, then it was counted as a non-failure. This check-point is located on the failure probability distribution (see Fig. 2.3) at line a-a. The area to the right of the line a-a was considered as the "High Strength Area". When the resistance was located in this area, it satisfied the pre-determined check-point, and the simulation counted as a non-failure.

This procedure was applied to a wood pole design with no

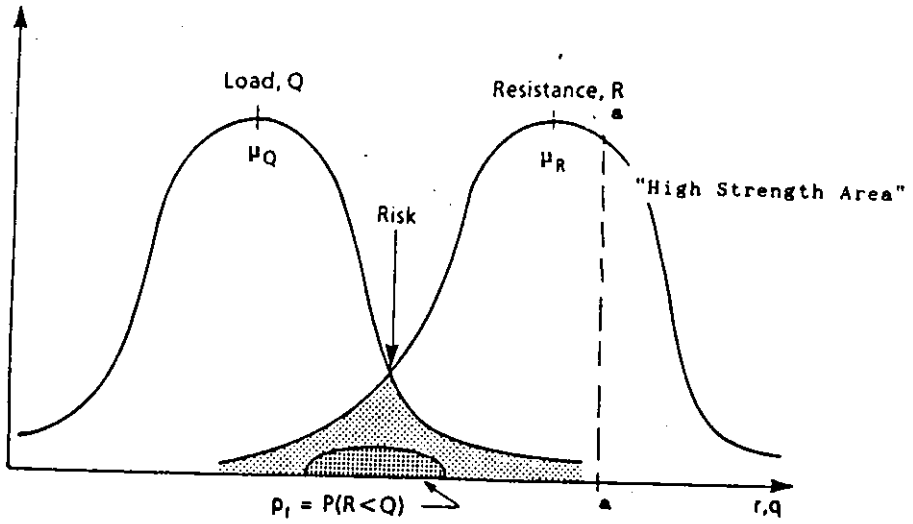

Fig. 2.3: Location of "High Strength Area" on failure probability distribution curves.

reduction in accuracy compared to an identical simulation that was performed without the censoring technique.

2.3.3.3 Finite element example

The next procedure utilizes the First Order-Second Moment (FOSM) method to calculate the probability of transmission line structural failure for a single structure. This method was applied to a 2-D transmission line tower with loading in the both the in-plane (vertical) and out-of-plane (horizontal) directions.

A.K. Haldar [17] proposed a finite element method which defined failure as a force in a member beyond its capacity. A member was specified as one of the components within an

individual transmission structure.

The equations used for the horizontal and vertical loadings due to combined wind and ice at the conductor attachment points are listed below:

$$P_H = \left[\frac{d_c + 2t}{12}\right] (G_F C_d) (0.00256 v^2) W_N \qquad (2.4)$$

$$P_V = [1.224 t (d_c + t) + w_c] W_T \qquad (2.5)$$

where,
P_H= horizontal load,
P_V= vertical load,
d_c= diameter of conductor,
t= ice thickness,
G_F= span reduction factor,
C_D= drag coefficient,
v= wind velocity,
W_N= wind span,
w_c= bare weight of conductor, and
W_T= weight span.

The finite element method utilized a first-order Taylor's series expansion to find the mean internal stress, S, and the standard deviation of the internal stress, σ_S, of each member in the transmission structure. The mean internal strength, R, was then derived from standard mechanics of materials equations, and the standard deviation of the internal strength, σ_R, was assumed.

A normal distribution was also assumed for these variables, (S, R, σ_S, σ_R), which were then used to calculate the probability of failure, $P_{f,i}$, of each member of the transmission structure by the following equation:
where ß is defined as the reliability index and $\Phi(-ß)$ can be

$$P_{f,i} = \phi\left[\frac{-(R-S)}{\sqrt{\sigma_R^2+\sigma_S^2}}\right] = \phi(-\beta) \qquad (2.6)$$

obtained from the standard normal table [17].

Then the $P_{f,i}$'s were combined to form lower and upper bounds, assuming total independence and total dependence, respectively, on the probability of failure of the structure in the next equation:

$$\max_i^M P_{f,i} < P_f < \sum_{i=1}^{M} P_{f,i} \qquad (2.7)$$

where P_f is the probability of failure of the structure, and M is the number of failure modes, or in this case, the number of members of the transmission structure.

This procedure was applied to an example transmission structure and sensitivity studies of the various input statistical parameters (e.g., loading, strength and sectional properties) were performed. One of the results of the analyses indicated that the failure probability of the structure increased by taking into account the effects of correlation between wind speed and ice thickness.

2.3.3.4 Plastic collapse failure example

A method proposed by Murotsu, Okada, Matsuzaki, and Nakamura [18] was specifically generated for the failures produced by large nodal displacements due to plastic collapse of the structure. This method was applied to a 2-D

transmission line structure similar to the structure in the previous example.

The load equations for this method were given for wind, snow and tension loads, in which the wind load, L_W, and snow load, L_S, are listed below:

$$L_W = \tfrac{1}{2} p\,(Gv)^2\, C_D\, (D+2t)\, S\, (H/10)^{1/4} \qquad \textbf{(2.8)}$$

$$L_S = \tfrac{\pi}{4}\left[(D+2t)^2 - D^2\right] p_s\, S \qquad \textbf{(2.9)}$$

where,

p= air density,
G= gust factor,
v= winter average wind speed at site of structure,
C_D= drag coefficient,
D= conductor diameter,
t= snow thickness,
S= span length,
H= height at which wind acts, and
p_s= snow density.

The tension loads, L_T, were determined by solving a non-linear equation which accounted for a maximum allowable stress of conductors, wind speed, snow thickness and temperature.

Then the horizontal and vertical loads acting on the conductor at its attachment point to the arms of the structure were calculated from L_W, L_S, L_T, and the angle of the conductors with respect to the surrounding structures.

A structural analysis using the direct displacement method was performed. For the given failure criteria and a transmission line structure with many degrees of redundancy, structural failure results only after the yielding of several

components within the transmission structure. To determine the system failure probability, one must investigate all possible failure mechanisms. However, this seems impractical to include all of these mechanisms, particularly in a highly redundant structure. Therefore, a procedure was used which selected the probabilistically significant failure paths. This selection process was accomplished with the branch-and-bound technique. For details related to this method, the reader is referred to Ref. 18.

This method was then successfully applied to a transmission line structure, and the dominant failure mode was found to be the side-sway mechanism of the top portion of the structure.

2.3.3.5 Newfoundland transmission line failure

Two major line failures occurred in 1980 and 1987 to the transmission line which runs along the west coast of Newfoundland. As a result, The Transmission Design Department of Hydro undertook a detailed study on the assessment of the existing line reliability and the course of action that is necessary to increase the level of reliability of the line [19].

The transmission tower of interest is a suspension-type, guyed-v tower, which means the structure is in the shape of the letter "V". The study included the analysis of the existing and upgraded structure under various basic climatic

loading conditions. The upgraded structure was improved by modifying some members to carry unbalanced vertical ice loads. The loading condition of unbalanced vertical ice loads was found to cause failure and contribute significantly to the probability of failure.

In this study, a total of nine load cases were considered. Seven of these load cases were related to ice-only loading while the remaining two load cases were extreme wind and combined wind and ice loads.

The strength of a member in the structure was taken to be a random variable and related to the nominal strength, R_n, as

$$R = MFPR_n \tag{2.10}$$

where,
- R= resistance,
- M= variability due to material,
- F= variability due to erection and fabrication,
- P= professional factor that represents the uncertainties in the strength theory, and
- R_n= nominal strength.

The variables M, R, and P were assumed to be uncorrelated random variables, so the coefficient of variation of the strength, V_R, could be approximated as:

$$V_R = \sqrt{V_M^2 + V_F^2 + V_P^2} \tag{2.11}$$

where,
- V_M= coefficient of variation of M,
- V_F= coefficient of variation of F, and

V_P= coefficient of variation of P.

In the reliability analysis of this work, some details of the procedure were not explained. The document states that interference between the strength, R, and stress, Q, (effects of various loads) was taken into account using the mathematical theory of probability [19]. From that point, the reliability of the tower R_{Tower} was computed based on the assumption that an individual member fails either in tension or in compression mode. Therefore, these two events are mutually exclusive under a particular load case. Members were grouped according to the particular mode of failure and total reliability of the structure was given as:

$$R_{Tower} = \left(\prod_{i=1}^{n} R_{ci}\right) \left(\prod_{j=n+1}^{m} R_{Tj}\right) \qquad (2.12)$$

where,

R_{ci}= reliability of an individual member, i, in compression,
R_{Tj}= reliability of an individual member, j, in tension,
m= total number of members under consideration.

Assuming the load case events are independent, the estimate of the structure lifetime failure probability was given by:

$$P_{f,T} = \sum_{i=1}^{M} P(N_i)\, P_{f,i} \qquad (2.13)$$

where,

$P_{f,i}$ = probability of failure given that the "load case i" occurs,
$P(N_i)$ = probability of occurrence of this load case, and
M = number of load cases.

The results of this analysis indicated that the existing structure has an annual probability of failure of 0.0096, or approximately 1 out of 100. The annual probability of failure for the upgraded structure was calculated to be 0.0073, or 7 out of 1000.

An economic analysis was also conducted in which the initial cost of the line is balanced against the future failure costs. The final results indicated that shortening of the existing span by adding structures is the most economical solution for upgrading this line.

The focus of this work is on the development of the limit state function, G{x}. The methods discussed in this chapter involve complicated equations and procedures to produce this equation. Development of the limit state function was accomplished in the next chapter, Chapter 3, by using a regression technique.

3. DESCRIPTION OF THE PROCEDURE

As shown in the previous chapter, numerous approaches to a reliability analysis have been documented. In this chapter, the method utilized to construct a fragility curve for a transmission line structure is developed. The calculation for the structure's probability of failure includes all possible failure modes that may affect the structure's performance. This analysis involves the following three steps:

1. Determination of the failure functions for possible failure modes.
2. Calculation of the probability of failure for each mode.
3. Combination of the individual modes failure probabilities to obtain the structure's probability of failure.

3.1 Development of the Failure Functions

A failure function defines the point at which a structural element fails to perform its function and is expressed as:

$$G = R\{x_i\} - Q \qquad (3.1)$$

where x_i represents the geometric and material variables that affect an element resistance, R, and Q is an applied load. The resulting magnitude of G{x} determines the presence of a safe or failure region. For example, G{x} > 0 indicates a safe region, and G{x} < 0 denotes a failure region.

Formulation of G{x} consists of using a closed form

solution. However, in most cases, this is a formidable task, particularly when dealing with complex systems such as transmission lines. Although some researchers have utilized finite element techniques (see Haldar [17] and Murotsu, et al. [18]), these techniques involve a significant number of rigorous analyses to incorporate the indeterminacy of the structure.

3.1.1 Generation of data points

Alternately, in the method proposed herein, G{x} can be derived by using a technique similar to a Monte Carlo simulation. This technique is advantageous because it does not require finite element analysis. In the following sections, the goal is to represent the failure regions with the minimum number of structural analyses and to use these representations to estimate the system failure probability. This method was developed using the principles described in Ref. 5.

In this procedure, a set of data points on the failure surface is estimated. The size of the set of data points is arbitrary but must have more data points then the number of variables in order for the regression analysis to be performed. Also a larger data set will result in a better estimate of the failure function. A regression technique is then employed to formulate the failure function. Estimation of the data points on the failure surface was accomplished

using two similar methods. The procedure of these two methods will be outlined in the example problems in Section 3.4.

3.1.2 Regression analysis

Regardless of the method of generating the data points, regression analysis is required to develop the limit state equation. Each group of data points associated with an individual failure mode were analyzed (or regressed) to determine the failure equation, G{x}, for each failure mode. The regression analysis was accomplished by using the statistical analysis program SAS [9]. This program uses the method of least squares to fit the generated equations. An example input file for the SAS program is presented in the following example in Section 3.4.1.

Each equation that was obtained was checked for independence between the residuals and the predicted values, and normality of the residuals. These checks confirm that the generated failure equation is an accurate representation of the data.

3.2 Reliability Analysis: First Order-Second Moment Method

As stated in the Chapter 2, the First Order-Second Moment (FOSM) method was used to calculate the probability of failure, P_f, for each possible failure mode, i.e.,:

$$P_f = P(G\{x\} \leq 0) \qquad (3.2)$$

3.2.1 Reliability index

The calculation of the probability of failure involves determination of a reliability index (often called the safety index), ß, defined as:

$$\beta = \frac{\mu_G}{\sigma_G} \tag{3.3}$$

where μ_G represents the failure function, G{x}, evaluated at the mean values of the variables, and σ_G is the standard deviation of G{x}. Equation 3.3 may also be expressed as

$$\mu_G - \beta \sigma_G \geq 0 \tag{3.4}$$

This is illustrated in Fig. 3.1 where the probability density function is shown for G. The shaded area to the left of the vertical axis is equal to the probability of failure. If the mean, μ_G, is moved to the right and σ_G is held constant, the probability of failure is reduced. Hence, increasing the value of ß corresponds to a reduction in failure probability or an increase in reliability.

The relationship between ß and the probability of failure, P_f, can be established by approximating the distribution of G{x} as a normal distribution [7], hence P_f can be calculated as:

$$P_f = \Phi(-\beta) \tag{3.5}$$

where Φ is the standard normal integral which can be estimated

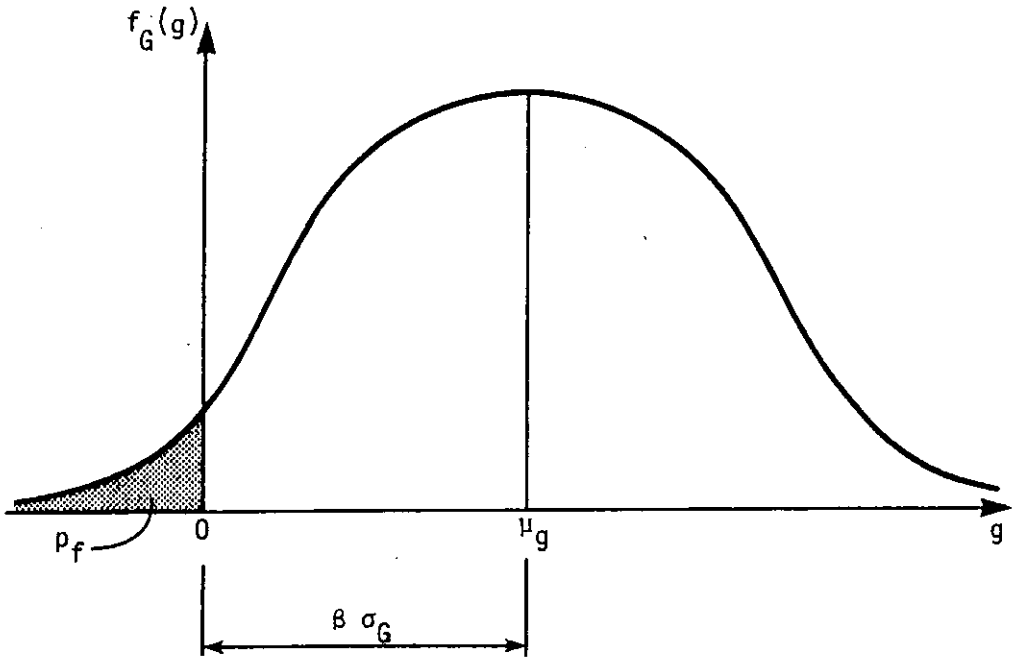

Fig. 3.1: Graphical illustration of reliability index.

the available normal distribution probability table. There are several techniques to calculate ß. In this research, the Lind-Hasofer method [7,8] was used. Details concerning this method are given in the next section.

3.2.2 Calculation of reliability index: Lind-Hasofer Method

When the failure function, G{x}, is non-linear, problems are encountered in calculating the safety index, ß. In this case, the FOSM methods account for the non-linearity by linearizing only a point on the failure boundary surface, referred to as the design point, $\{x^*\}$. The procedure is iterative and involves recalculating the design point several times and linearizing G{x} at each point.

The Lind-Hasofer method is used in this study since it is the basis for most methods [6]. This method can be described in two steps: (1) transformation of the random variables, {X}, into a space of reduced variables, {Y}, by

$$\{\sigma_X\}\{Y\} = \{X\} - \{\mu_X\} \tag{3.6}$$

and (2) measuring, in the transformed space, the shortest distance between the origin of the space to the failure surface. This concept is illustrated in Fig. 3.2 for a two-parameter failure function.

The reliability index, ß, is defined as the minimum distance between the origin and the failure surface in the transformed space. The design point now becomes $\{y^*\}$ and represents the "most likely" point of failure. Calculating the design point requires solving a minimization problem. A numerical solution is defined by the following system of equations, with respect to the original variable space of independent random variables, {X},

$$\{\alpha\} = \lambda\,[\sigma_X]\,\{\nabla G\} \tag{3.7}$$

$$\{x^*\} = \{\mu_X\} - \beta\,[\sigma_X]\,\{\alpha\} \tag{3.8}$$

$$G\{x^*\} = 0 \tag{3.9}$$

$$\lambda = [\{\nabla G\}^T [\sigma_X^2]\,\{\nabla G\}]^{-1/2} \tag{3.10}$$

in which {∇G} are the gradients of G evaluated at the design

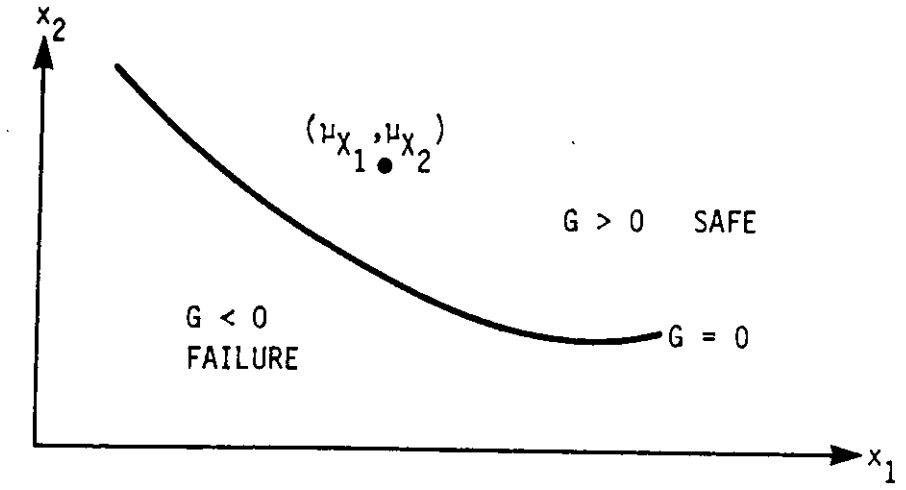

a.) ORIGINAL COORDINATES

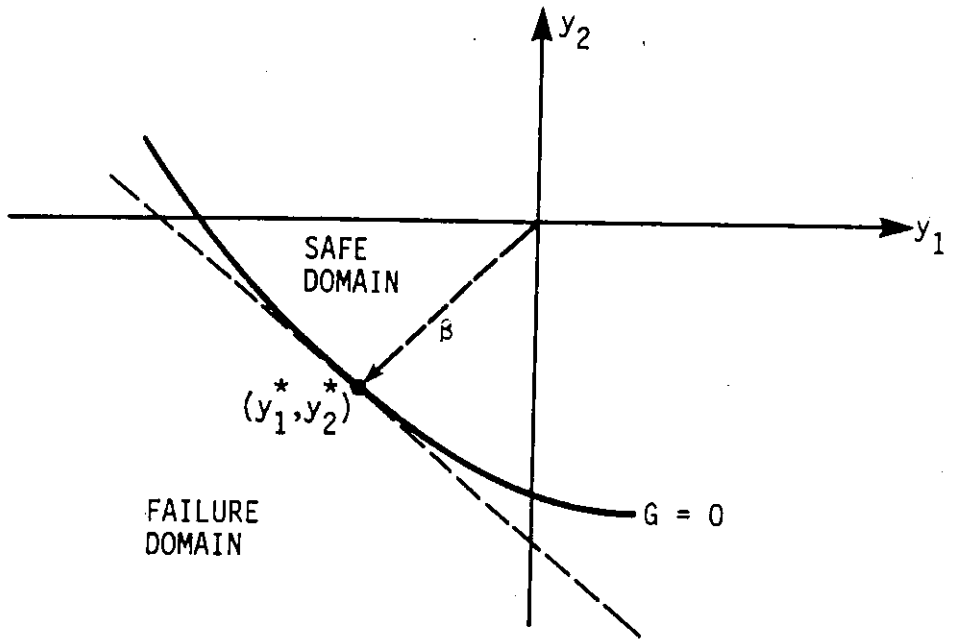

b.) REDUCED COORDINATES

Fig. 3.2: Original and reduced variable coordinates in reliability analysis.

point $\{x^*\}$, and $\{\alpha\}$ is the vector containing the direction cosines of the random variables.

The Lind-Hasofer method is slightly modified to account for random variables with non-normal distributions. This can be accomplished by transforming the non-normal variables into reduced normal variables prior to the solution of the minimization problem [7]. The transformation process involves the determination of the mean and standard deviation of an equivalent normal variable, $\mu_{xi}{}^N$ and $\sigma_{xi}{}^N$. These are found under the conditions that the cumulative distribution and probability density function of the non-normal and approximating normal variable are equal at the design point, $\{x^*\}$. This leads to:

$$\sigma_{X_i}^N = \frac{\phi(\phi^{-1}[F_{X_i}(x_i^*)])}{f_{X_i} x_i^*} \qquad (3.11)$$

$$\mu_{X_i}^N = x_i^* - \phi^{-1}[F_{X_i}(x_i^*)]\,\sigma_{X_i}^N \qquad (3.12)$$

where $F_{Xi}(.)$ and $f_{Xi}(.)$ denote the actual cumulative distribution and density distribution of the non-normal variable, X_i.

An iterative procedure to calculate the reliability index, ß, is summarized in Ref. 7 as follows:

1. Define the limit state function [Eq. (3.1)].
2. Approximate an initial value of the reliability index, ß.

3. Set the initial design point values $\{x^*\} = \{\mu_x\}$.

4. Compute $\mu_{xi}{}^N$ and $\sigma_{xi}{}^N$ for those variables that are non-normal according to Eqs. (3.10) and (3.11).

5. Calculate partial derivatives, $\{\nabla G\}$, evaluated at the design point, $\{x^*\}$.

6. Compute the direction cosines, $\{\alpha\}$, from Eq. (3.6).

7. Compute new values of $\{x^*\}$ from Eq. (3.7) and repeat steps 4 through 7 until estimates of $\{\alpha\}$ stabilize.

8. Compute the value of ß necessary for $G\{x^*\} = 0$.

9. Repeat steps 4 through 8 until the values of ß on successive iterations are within an allowable tolerance.

When a satisfactory value of the minimum distance, ß, is obtained, the failure probability, P_f, can be evaluated from $\Phi(-\beta)$.

3.3 Multiple Failure Functions

The previous sections describe the generation of the failure functions, G{x}, and the calculation of the probability of failure from G{x}. In this section, the computation of the structural probability of failure is discussed.

Once the failure modes and associated probabilities are established, the system probability of failure is calculated. This computation involves the statistical union (U) of the individual modes of failure, i.e., the system failure probability can be expressed as:

where n is the number of failure modes.

$$P_f = P[(G_1 \le 0) \cup (G_2 \le 0) \cup \ldots \cup (G_n \le 0)] \qquad (3.13)$$

The exact calculation of P_f requires the determination of the correlations between all of the failure modes. If more than two failure modes are considered, calculating the correlations, and incorporating it into the probability of failure equations is a tedious task. Therefore, simplifications are employed to calculate upper and lower bounds instead of the exact probability. For example, assuming that independence among the failure modes, the upper bound failure probability is:

$$P_f^U = 1 - \prod_{i=1}^{n} \{1 - P[F_i]\} \qquad (3.14)$$

for small $P[F_i]$, the formula may be simplified to

$$P_f^U = \sum_{i=1}^{n} P[F_i] \qquad (3.15)$$

The lower bound failure probability is calculated based on the assumption that the failure modes are dependent on each other which corresponds to the largest failure probability among the individual modes. The lower bound failure probability is shown below as:

$$P_f^L = \max P[F_i] \qquad (3.16)$$

For a large and complex structure, derivation of all of the failure modes including the modes that have a very small

probability of occurring, may be very time consuming. Therefore, one may consider only the dominant failure modes. This will not significantly jeopardize the calculation of the system calculation of the probability of failure. This will be illustrated in the ten-bar truss example in the next section, Section 3.4.2.

3.4 Examples Problems

3.4.1 Ten-bar truss

In this technique, an iterative process to obtain a set of data points is used. The procedure consists of increasing the applied loads until a component in the structure reaches its structural ultimate strength. The structure is then modified by constraining the forces of the failed component to its estimated ultimate strength and reanalyzing the system to predict the next component to fail. These steps are repeated until a system failure is attained.

This process also involves random generation of the system variables that define the strength of all structural members. Assuming a normal distribution, a random generator that utilizes the mean and standard deviation can be used to generate random values for the system variables. This step was accomplished using the normal random number generator in the Minitab software statistical program [21]. Minitab is also capable of generating random numbers with other

distributions such as the Weibell and Poisson distributions.

The proposed method is a simulation technique but differs from Monte Carlo simulation. The simulation runs in this method are used to formulate the limit state, whereas in a Monte Carlo simulation the probability of failure is directly calculated. Also, the number of analyses in Monte Carlo simulation (in the range of 10,000) greatly exceeds the number of analyses used for this method (in this case 29).

To demonstrate this procedure the ten-bar truss system, shown in Fig. 3.3 [8,22], was used. The basic variables in this example are the individual element resistances which are considered statistically independent and characterized by a normal distribution. The mean values of each element resistance, R_i, are listed in Table 3.1. A coefficient of variation for each element resistance is assumed as 0.2.

Component failure results when the axial load in the member reaches the member ultimate capacity leading to failure. System failure occurs when the structure reaches an unstable stage. One should notice that failure of elements 1, 3, 7, or 10 result in an unstable structure and hence a system failure. Therefore, the analysis is a lot simpler and must be concluded when any of these members fail.

Reliability analyses of the ten-bar truss was accomplished by analyzing the structure 29 times. Each of the 29 analyses resulted in one of five failure modes. Overall,

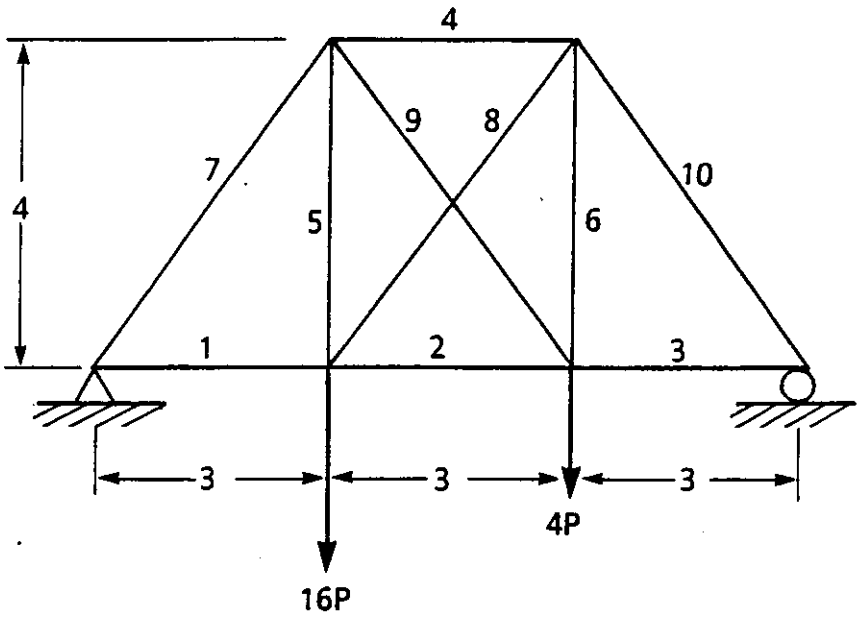

Fig. 3.3: Ten-bar truss example problem.

Table 3.1: Mean resistances for the truss elements in Fig. 3.3.

ELEMENT NUMBER	ELEMENT MEAN RESISTANCE (kips)
1	15
2	15
3	15
4	15
5	20
6	20
7	25
8	10
9	10
10	25

there was approximately six analyses (or six data points) for each failure mode.

For each structural analysis, a random number was generated for all of the elements' resistances utilizing the member mean and coefficient of variation in conjunction with the Minitab software [21]. For example, the element resistances for one of these 29 analyses are listed below:

R_1 = 12.61 kips, R_4 = 13.19 kips, R_5 = 12.99 kips,
R_7 = 30.11 kips, R_8 = 9.82 kips

For the listed resistances, the value of P (see Fig. 3.3) was determined by first conducting a structural analysis which indicated that element number 5 will reach its resistance as P reaches 1.18 kips.

The structure was then modified so that the force in element 5 was constrained to 12.99 kips. The analysis was continued by increasing the value of P until another element(s) failed. In this example, it was determined that element 4 would reach its capacity as the value of P reaches 1.27 kips. No further analysis could be performed since failure of element 4 results in an unstable structure.

The data points associated with a particular failure sequence are grouped together. For the current example, there were five failure modes. The five failure modes and the respective variables used to identify the limit state equation for each failure mode are listed below:

* failure of element 1 denoted by $G_1\{x\}$

* failure of element 7 denoted by $G_7\{x\}$
* failure of elements 4 and 5 denoted by $G_{4,5}\{x\}$
* failure of elements 5 and 8 denoted by $G_{5,8}\{x\}$
* failure of elements 4 and 8 denoted by $G_{4,8}\{x\}$

The list of generated data points is located in Table 3.2 in which the data points are grouped by failure modes. Regression analysis of each group of data points was performed using the SAS software [9]. An example SAS program for the calculation of the limit state equation, $G_{4,5}\{x\}$, is located in Fig. 3.4. This program include the data points which are highlighted in Table 3.2. The output from this program is shown in Fig. 3.5 and can be interpret by taking note of the figures indicated in Fig. 3.5. These figures are the estimates of the coefficients for the corresponding variables as denoted in the "Parameter" column, which is also indicated in Fig. 3.5. The SAS program computes the equation:

$$P = 0.0555694124\,X_4 + 0.0416708885\,X_5 \qquad \textbf{(3.17)}$$

The limit state equation has all the variables on one side of the equation, so rearranging and rounding of the variables results in the limit state equation for failure of elements 4 and 5 as:

$$G_{4,5}(x) = 0.0556\,R_4 + 0.0417\,R_5 - P \qquad \textbf{(3.18)}$$

The equations for the remaining failure modes are calculated in the same manner and are listed below:

Table 3.2: Data points for ten-bar truss example.

P (kips)	R_1(kips)	R_4(kips)	R_5(kips)	R_7(kips)	R_8(kips)
FAILURE OF ELEMENT 1					
1.16	10.40	12.75	22.85	25.29	8.05
0.96	8.64	16.70	21.05	30.09	7.93
0.98	8.80	12.61	12.99	30.11	9.82
1.09	9.82	16.42	20.56	28.09	8.61
1.11	9.99	14.52	16.79	28.42	11.43
1.44	12.99	17.65	20.29	40.22	11.03
FAILURE OF ELEMENT 7					
1.38	18.00	16.09	18.41	20.67	10.11
1.28	20.24	17.79	17.77	19.19	8.38
1.12	14.83	22.18	21.54	16.84	8.51
1.41	18.15	13.30	25.40	21.21	10.00
1.38	18.85	19.06	22.78	20.62	12.65
1.50	27.13	20.95	20.72	22.56	13.07
FAILURE OF ELEMENTS 4 AND 5					
1.27	12.61	13.19	12.99	30.11	9.82
1.44	16.42	10.49	20.56	28.09	8.61
1.43	14.52	13.07	16.79	28.42	11.43
1.58	17.65	13.16	20.30	40.22	11.03
1.58	15.67	14.80	18.12	31.30	12.28
1.72	20.52	13.22	23.59	26.97	11.45
1.67	18.46	13.85	21.54	30.42	8.51
FAILURE OF ELEMENTS 5 AND 8					
1.49	15.00	15.00	15.90	25.00	10.0
1.66	16.45	20.07	18.41	25.89	10.11
1.53	20.71	15.40	17.77	30.29	8.38
1.66	14.94	17.59	25.40	31.87	10.00
1.71	19.36	17.39	18.78	25.97	10.65

Table 3.2 (cont.)

P (kip)	R_1 (kip)	R_4 (kip)	R_5 (kip)	R_7 (kip)	R_8 (kip)
FAILURE OF ELEMENTS 4 AND 8					
1.61	15.00	15.00	20.00	25.00	8.90
1.38	12.75	13.12	22.85	25.29	7.05
1.32	16.70	12.69	21.05	30.09	7.93
1.48	13.78	14.22	18.46	23.85	8.92
1.76	17.01	15.20	22.28	27.06	7.78

```
// JOB
//SAS EXEC SAS
//DD SYSIN **

DATA FAIL45;
     INPUT P X4 X5;

     CARDS;

1.27        13.19       12.99
1.44        10.49       20.56
1.43        13.07       16.79
1.58        13.16       20.29
1.59        14.80       18.12
1.71        13.22       23.59
1.67        13.85       21.54
;

PROC GLM;
     MODEL P=X4 X5;
     OUTPUT OUT=NEW PREDICTED=YHAT RESIDUAL=RESID;

PROC PLOT; PLOT RESID*YHAT;

PROC SORT; BY RESID;
DATA NPLOT; SET NEW;
N+2; NS=PROBIT((N-1)/14);

PROC PLOT; PLOT NS*RESID;
```

Fig. 3.4: SAS program used to perform regression analysis.

General Linear Models Procedure

Dependent Variable: P

Source	DF	Sum of Squares	Mean Square	F Value	Pr > F
Model	2	0.14257569	0.07128784	99999.99	0.0001
Error	4	0.00000000	0.00000000		
Corrected Total	6	0.14257569			

R-Square	C.V.	Root MSE
1.000000	0.001011	0.00001543

Source	DF	Type I SS	Mean Square	F Value	Pr > F
X4	1	0.01740105	0.01740105	99999.99	0.0001
X5	1	0.12517464	0.12517464	99999.99	0.0001

Source	DF	Type III SS	Mean Square	F Value	Pr > F
X4	1	0.03116393	0.03116393	99999.99	0.0001
X5	1	0.12517464	0.12517464	99999.99	0.0001

Parameter	Estimate	T for H0: Parameter=0	Pr > |T|	Estimate
INTERCEPT	-.0002481606	-3.24	0.0317	0.00007660
X4	0.0555694124	11443.77	0.0001	0.00000486
X5	0.0416708885	22935.13	0.0001	0.00000182

Fig. 3.5: Output from SAS program in Fig. 3.4 used to develop the limit state equation, $G_{4,5}\{x\}$.

$$G_1\{x\} = 0.111R_1 - P \qquad (3.19)$$

$$G_7\{x\} = 0.067R_7 - P \qquad (3.20)$$

$$G_{5,8}\{x\} = 0.0624R_5 + 0.05R_8 - P \qquad (3.21)$$

$$G_{4,8}\{x\} = 0.1624R_4 + 0.101R_8 - P \qquad (3.22)$$

Knowing the failure function for each mode, one can calculate the probability of failure, P_f, utilizing the FOSM method (see Section 3.2). A spreadsheet was used to for these

calculations which is shown in Fig. 3.6. The spreadsheet shown was used for the failure equation, $G_{4,5}\{x\}$. Under the heading "ENTERED PARAMETERS", the value for the load, in this case P, is entered. Then the initial guess for beta is entered. Convergence of the "Alpha_*xx*" variables indicate that no more iterations are required. This spreadsheet shows three iterations, which is all that is necessary in this example, but for more complicated equations, more iterations may be necessary. After the "Alpha_*xx*" variables converged,

EQUATION: G(X) = 0.0556 X_4 + 0.0417 X_5 - P

DEFINITION OF VARIABLES **********

MEAN_X4	15	SIGMA_X4	3
MEAN_X5	20	SIGMA_X5	4

****

EQUATION VARIABLES **********

CONSTANT	0
X4	0.0556
X5	0.0417

****

ENTERED PARAMETERS **********

P = 1

Initial Beta = 2.83

CALCULATED BETA **********

BETA= 2.83

CALCULATIONS **********

X_4*	15	X_4*	9.00	X_4*	9.00
X_5*	20	X_5*	12.00	X_5*	12.00
dG/X4	0.0556	dG/X4	0.0556	dG/X4	0.0556
dG/X5	0.0417	dG/X5	0.0417	dG/X5	0.0417
Lamba=	4.2392	Lamba=	4.2392	Lamba=	4.2392
Alpha_X4	0.7071	Alpha_X4	0.7071	Alpha_X4	0.7071
Alpha_X5	0.7071	Alpha_X5	0.7071	Alpha_X5	0.7071
FIRST ITERATION		SECOND ITERATION		THIRD ITERATION	

****

Fig. 3.6: Spreadsheet for calculation of beta.

then the task is to change the "Initial Beta" until it converges with the calculated "BETA". For a linear equation such as $G_{4,5}\{x\}$, the "Initial Beta" does not alter the calculation of "BETA", but for more complex equations, this step is necessary.

The bounds of the failure probability can then be estimated using Eqs. (3.15) and (3.16) (see Sections 3.3). The results of this analysis are compared to the results obtained by Knapp [8] who used 19 failure modes (see Fig. 3.7).

The proposed method to calculate a system failure probability while considering fewer failure modes proves to be close to the estimations obtained in [8]. This demonstrates that one needs to use only the dominate failure modes to obtain the fragility curve for the structure.

In the technique demonstrated above, the user needs not know the failure sequence prior to analyzing a structure. Therefore, in order to group together enough data points for a specific failure mode, the values of some of the randomly generated variables can be "directed", (i.e. weakened or strengthened). More specifically, the weakening or strengthening of a variable means that the mean value is increased or reduced in the random number generator as a way of forcing certain failure paths.

The use of the "directing" technique does not guarantee

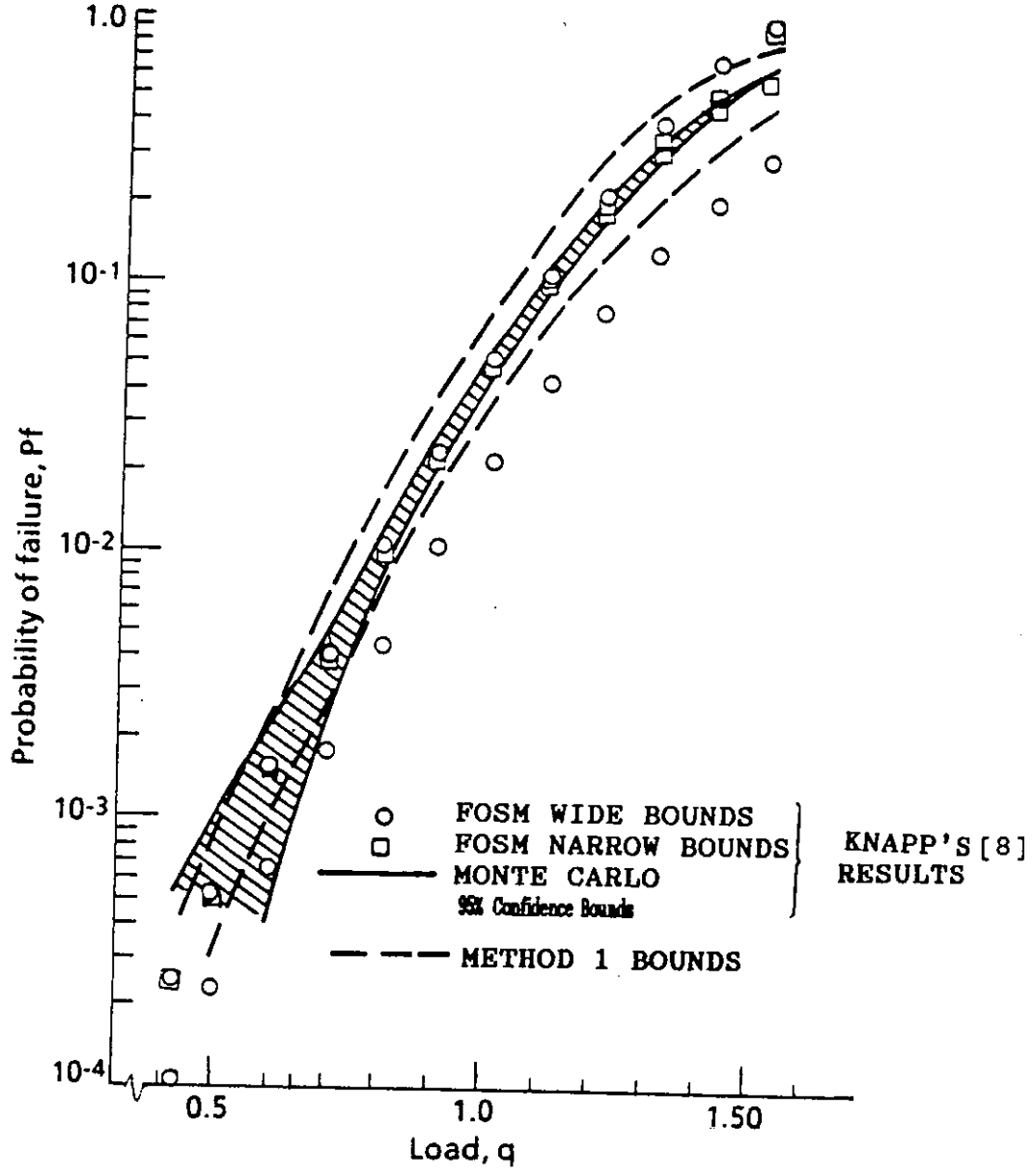

Fig. 3.7: Fragility curve for ten-bar truss example.

that all failure modes with high-probability will be identified and included in the analysis. This is a disadvantage of this procedure. Also the user is expected to interpret the information from the structural and statistical analyses and to recognize which elements to "direct" either by weakening or strengthening. As a result of this disadvantage, the technique listed below was examined, which is a more systematic way to identify the failure modes.

3.4.2 Portal frame

This approach for generating data points on the failure surface is more specific than Method 1. Instead of generating resistance variables, the applied loads were randomly generated. Then, the structural analyses were performed, and the resulting member forces were recorded.

The user determines the failure modes needed for estimating the system reliability. In contrast to the previous method (Method 1), the failure modes were unknown prior to the completion of all the analyses. Some simulations using Method 1 resulted in modes that were not included in the probability of failure calculation. Method 2 eliminates those structural analyses; therefore, less simulations were necessary to accumulate enough data points for the same failure mode.

(The 29 analyses cited in Section 3.4.1 did not include the extra analyses which did not contribute information to the

example. Since the time for each structural analysis for that example is so insignificant, the irrelevant analyses were disregarded instantaneously and a count of them was not possible.)

The above procedure (Method 2) is first demonstrated, then verified. The demonstration utilized the portal frame shown in Fig. 3.8 [8]. Verification of Method 2 was also conducted using the previous ten-bar truss example.

In the portal frame example, elastic-perfect plastic material properties were assumed. Structural failure is defined when a collapse mechanism is formed. The random variables are the loads, P_1 and P_2, and the plastic moment capacity of each element is R_i. The variable, R_i is the plastic capacity of the section located at the joints in Fig. 3.8. The mean values and coefficient of variation for these variables assuming a normal distribution are listed in Table 3.3.

The first step was to identify the failure sequence. For example, Fig. 3.9 shows all the possible failure mechanisms for the portal frame in Fig. 3.8. To illustrate this method, the mechanism involving the beam failure (i.e., the formation of plastic hinges at location 2, 4, and 7) was considered.

Next, random loads were generated for P_1 and P_2 using Minitab [21] (see Table 3.4). Ten values were generated for ten analyses. The loads were used to analyze the portal frame

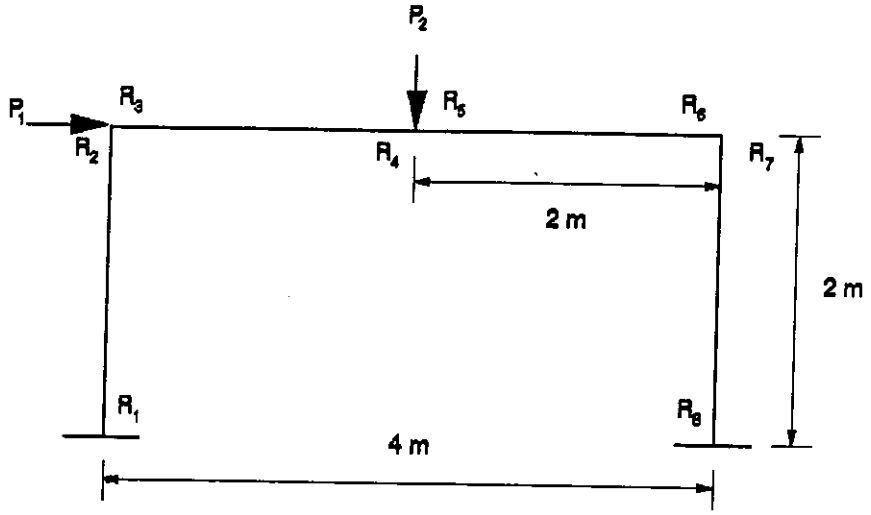

Fig. 3.8: Portal frame example.

Table 3.3: Mean values of the random variables for the structure in Fig. 3.8.

VARIABLE	MEAN	C.O.V.
P_1	20 kN	0.05
P_2	40 kN	0.05
R_1, R_2	75 kN*m	0.30
R_3, R_4, R_5, R_6	101 kN*m	0.30
R_7, R_8	75 kN*m	0.30

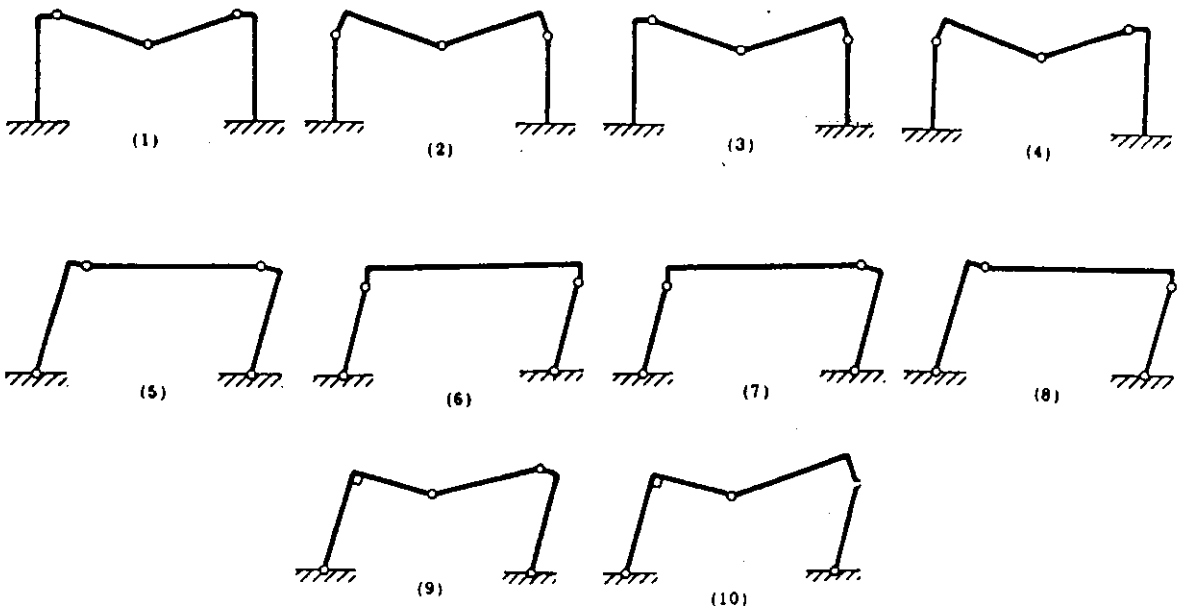

Fig. 3.9: Failure mechanisms for portal frame.

Table 3.4: Random numbers generated for P_1 and P_2.

Analysis	P_1 (kN)	P_2 (kN)
1	20.00	40.00
2	19.86	48.72
3	21.41	35.12
4	22.83	25.27
5	17.69	48.50
6	28.39	35.49
7	13.41	43.57
8	11.75	47.18
9	21.22	25.60
10	23.09	19.90

for the first iteration. The structure was then modified by introducing a hinge and a moment at locations 2, 4 or 7 where the largest of the three moments occurred. In this case, the evaluation illustrated that the first hinge will occur at location 7. The structure was then modified by introducing a hinge and a moment at location 7 (see Fig. 3.10). This is the ultimate capacity of the member at this location and was assumed to be varied for each analysis, so it was defined by the value calculated from this iteration. For example, considering Analysis 1 where P_1=20 kN and P_2=40 kN, the moment at hinge 7 was 57.44 kN*m, so this was the value of the R_7 in Fig. 3.10.

For the second iteration, the modified structure was subjected to loads P_1, P_2 and R_7 with the values shown in Table 3.5. The loads P_1 and P_2 were increased by an arbitrary amount of 2 kN from the first iteration; while R_7 was kept

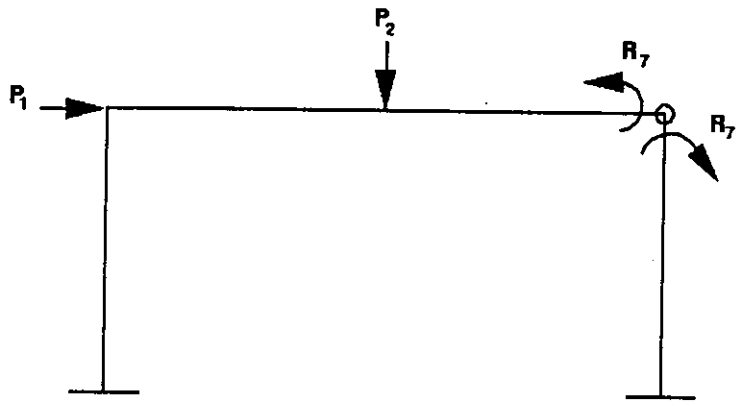

Fig. 3.10: Modified structure for second iteration.

Table 3.5: Applied loads to structure in Fig. 3.10.

Run	P_1 (kN)	P_2 (kN)	R_7 (kN*m)
1	22.00	42.00	57.44
2	21.86	50.72	65.47
3	23.41	37.12	54.28
4	24.83	27.27	46.47
5	19.69	50.50	63.10
6	30.39	37.49	61.60
7	15.41	45.57	54.15
8	13.75	49.18	55.92
9	23.22	27.60	45.17
10	25.09	21.90	41.69

constant. After the analysis of the modified structure was completed, the structure was then modified by introducing another hinge at location 4. The evaluation indicated that location 4 was the next plastic hinge location. Considering only Analysis 1 again, the moment was constrained at this location to 67.83 kN*m (see Fig. 3.11).

For the final step, the structure shown in Fig. 3.11 was subjected to P_1 and P_2 with the values shown in Table 3.6. Loads P_1 and P_2 were increased again from the previous iteration, while R_4 and R_7 remained the same, and the moment at location 2 was monitored.

Regression of the data points in Table 3.7 was used to develop the limit state equation as described in Section 3.1.1. Each row in Table 3.7 consists of one data point. The

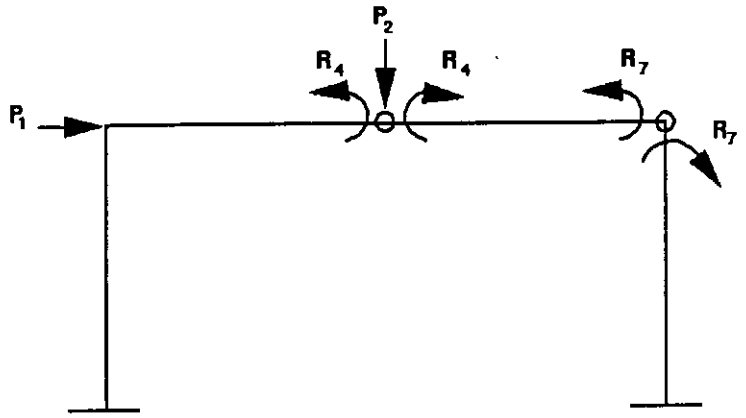

Fig. 3.11: Modified structure for third iteration.

Table 3.6: Applied loads to structure in Fig. 3.11.

Run	P_1 (kN)	P_2 (kN)	R_7 (kN*m)	R_4 (kN*m)
1	32.00	52.00	57.44	67.83
2	31.86	60.72	65.47	81.46
3	33.41	47.12	54.28	60.21
4	34.83	37.27	46.47	44.82
5	29.69	60.50	63.10	81.12
6	40.39	47.49	61.60	60.79
7	25.41	55.57	54.15	73.44
8	23.75	59.18	55.92	79.04
9	33.22	37.60	45.17	45.32
10	35.09	31.90	41.69	36.41

Table 3.7: Data points for beam mechanism failure mode for portal frame example.

P_1 (kN)	P_2 (kN)	R_2 (kN*m)	R_4 (kN*m)	R_7 (kN*m)
32.00	52.00	66.90	67.83	57.44
31.86	60.72	75.21	81.46	65.47
33.41	47.12	60.92	60.21	54.28
34.83	37.27	50.26	44.82	46.47
29.69	60.50	77.18	81.12	63.10
40.39	47.49	54.28	60.79	61.60
25.41	55.57	76.83	73.44	54.15
23.75	59.18	81.88	79.04	55.92
33.22	37.60	52.19	45.32	45.17
35.09	31.90	44.98	36.41	41.69

regression analysis resulted with the following failure equation, $G_{7,4,2}\{x\}$:

$$G_{7,4,2}\{x\} = R_7 + 2.01R_4 + R_2 - 5.01P_2 \qquad \textbf{(3.23)}$$

By comparison, the failure equation, $G'_{7,4,2}\{x\}$, listed in[8] for this mode of failure is:

$$G'_{7,4,2}\{x\} = R_7 + 2R_4 + R_2 - 5P_2 \qquad \textbf{(3.24)}$$

which indicated that the procedure developed herein is capable of reproducing the same failure equation, and validates Method 2.

Another validation of Method 2 was accomplished using the previous ten-bar truss example. The limit state equation, $G_{4,5}\{x\}$, for the failure of elements 4 and 5 shown in Eq. (3.18) was derived utilizing Method 1. The limit state

function for the same failure mode was again developed using Method 2. This failure equation, $G_{4,5}\{x\}$, was calculated as:

$$G_{4,5}\{x\} = 0.0556\,R_4 + 0.0417\,R_5 - P \qquad \textbf{(3.25)}$$

Comparing Eqs. (3.18) and (3.25) reveals that methods 1 and 2 are the same.

4. ANALYSIS OF A TYPICAL TRANSMISSION LINE

The procedure outlined in the previous chapter was applied to develop a fragility curve for one structure of the recently failed Lehigh-Sycamore transmission line [3]. The structure chosen was Tower 281. This tower is one of several structures that were damaged on October 31, 1991 when a severe ice storm hit the central part of the state of Iowa (for more detail, see Chapter 1).

To construct the fragility curve for the failed structure under ice loading, a computer model was used to analyze a portion of the transmission line utilizing the ETADS [2] software. The results were then used in the reliability analysis previously summarized to estimate the failure probabilities associated with the different failure modes. Buckling of the pole, plastic collapse of the pole and cross arms and insulator failure were considered.

4.1 Finite Element Model

In previous work [1,3], detailed models of transmission lines consisting of several structures were used to analyze failed transmission lines to estimate the failure loads. In this study, a similar but simplified model was utilized. The model used included only one tower on each side of Tower 281 and is referred to hereafter as Model 1 (see Fig. 4.1). This is only an approximate model of a transmission line segment,

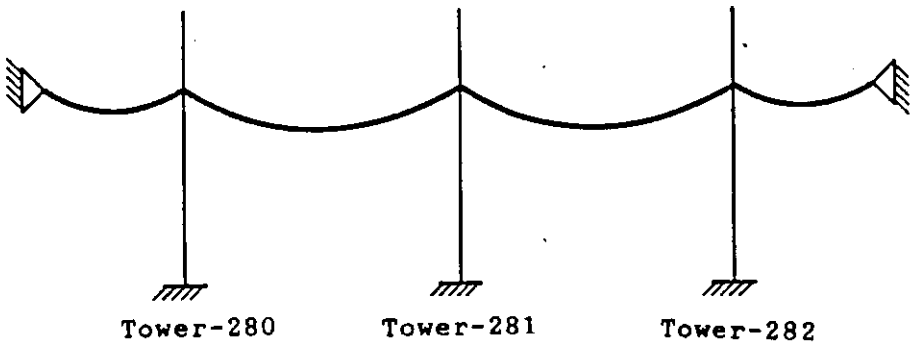

Fig. 4.1: Model 1 computer model.

but is only used to demonstrate a reliability analysis. However, if more accurate results are desired, a transmission line model that includes more structures must be used [3].

In idealizing the structures shown in Fig. 4.1, a fine mesh of elements was used to model Tower 281. A large displacement elastic analysis was performed. Linear material behavior was considered to reduce the computational time.

The effects of material nonlinearity was included in a model that consisted of one structure. This model is referred to hereafter as Model 2. In this model, the conductor was excluded and the forces at the conductor-insulator connections obtained from analyzing Model 1 were used as input to analyze Model 2.

4.2 Modelling Assumptions of the Transmission Line System

4.2.1 Geometry

Figure 4.2 illustrates a typical transmission line structure of the failed line. The towers are H-frame

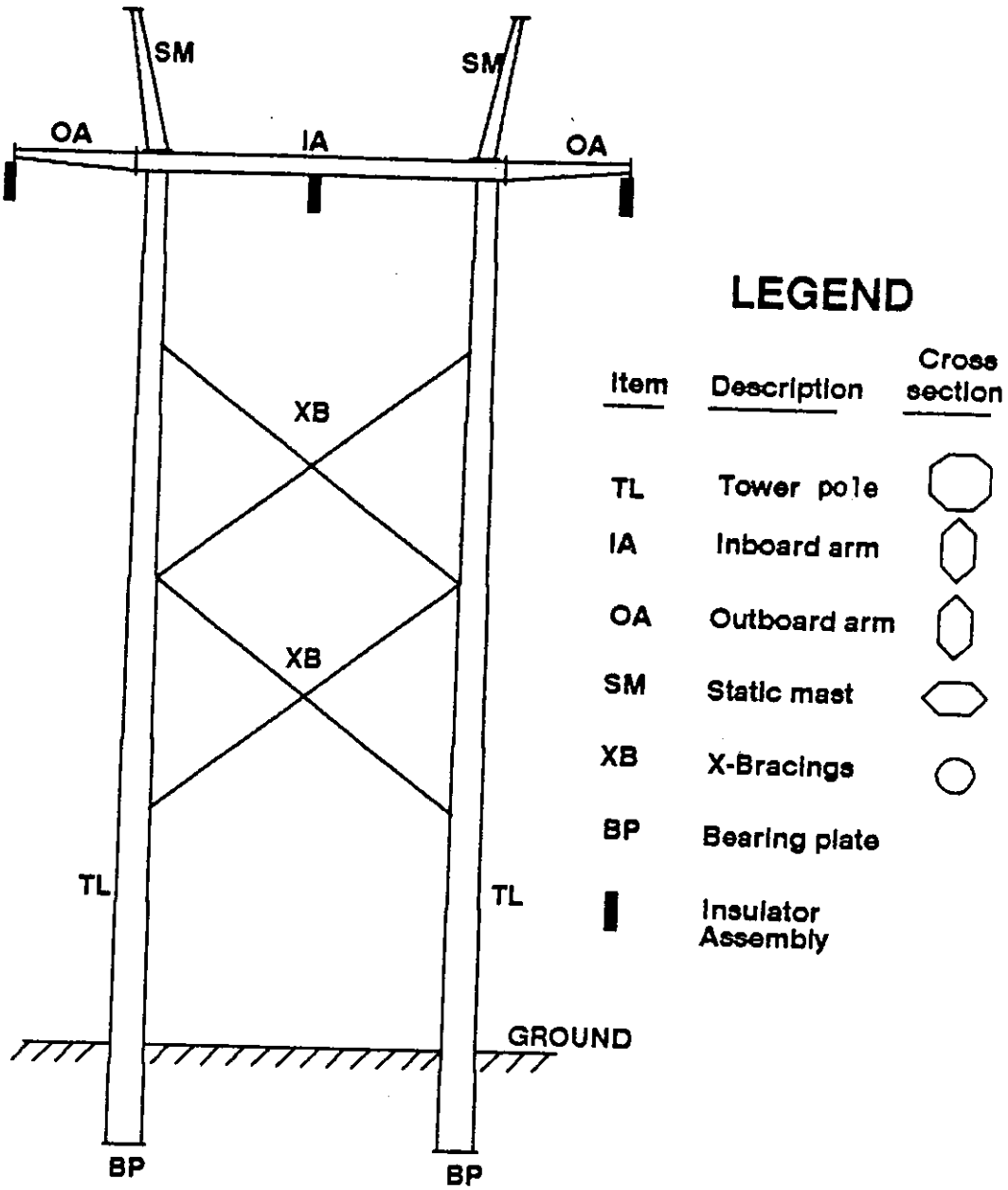

Fig. 4.2: A typical transmission line structure.

structures built using hollow tubular steel members. The structure was assumed to have a fixed base support at the ground level.

The dimensions and cross-sectional properties for Tower 281 are illustrated in Fig. 4.3 and Fig. 4.4. However, the hexagonal section of the cross-arm was idealized in the model with an equivalent uniform octagonal section with the same inertia and cross-sectional area.

The insulator assembly is shown in Fig. 4.5. This assembly consists of several hardware components with varying cross-sectional dimensions. Because the insulator units are allowed to rotate relative to another, its flexural stiffness was neglected in the finite element model. Hence, these insulators were modelled as catenary cable elements.

Figure 4.6 illustrates the joint where the inboard arm, outboard arm, static mast and the tower pole are connected. This complex joint was simplified in the finite element idealization assuming a rigid connection also shown in Fig. 4.6.

A plan view of one span showing the conductors and shield wires modelled in Model 1 is illustrated in Fig. 4.7. The figure shows that there were three groups of conductors corresponding to three phases and two shield wires in each of the spans. The bundled conductor for each phase had two conducting wires attached to the structure insulators through

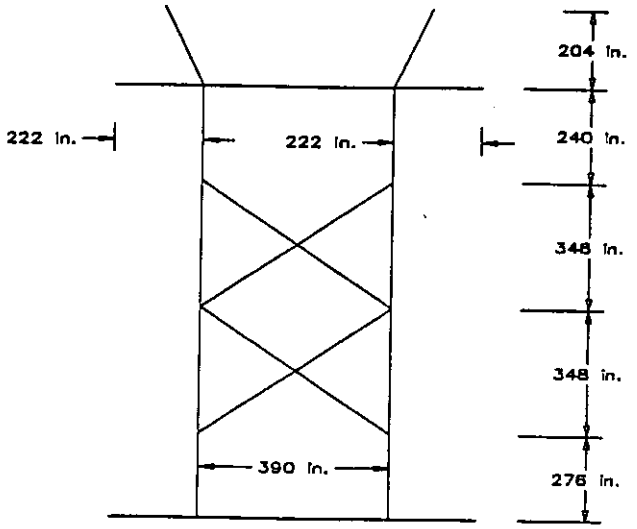

Fig. 4.3: Dimensions for Tower 281.

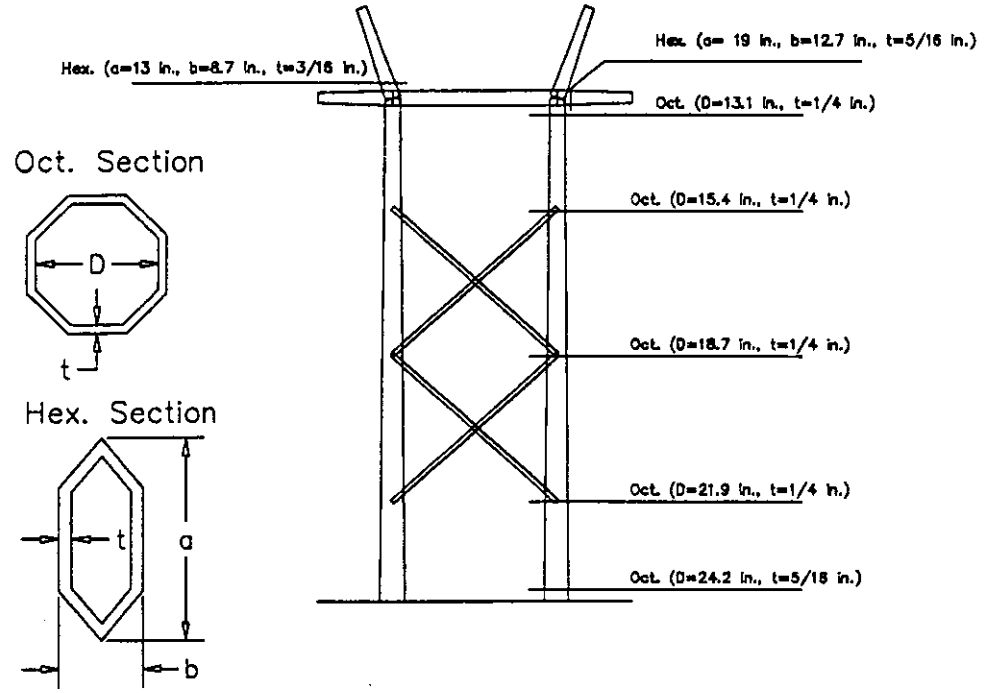

Fig. 4.4: Cross-sectional properties for Tower 281.

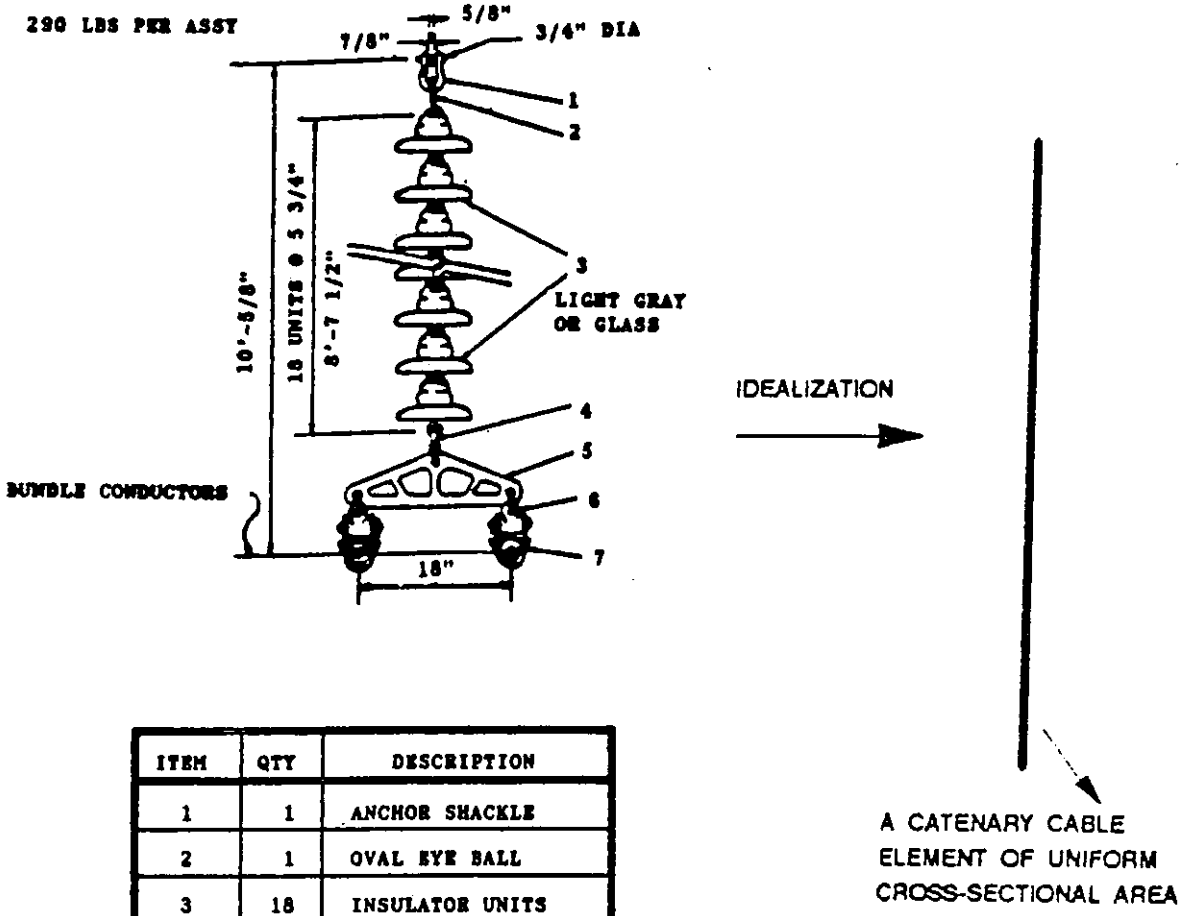

ITEM	QTY	DESCRIPTION
1	1	ANCHOR SHACKLE
2	1	OVAL EYE BALL
3	18	INSULATOR UNITS
4	1	SOCKET "Y" CLEVIS
5	2	EYE "Y" CLEVIS
6	2	SUSPENSION CLAMP
7	1	YOKE PLATE

Fig. 4.5: A typical insulator assembly and its idealization in the finite element model.

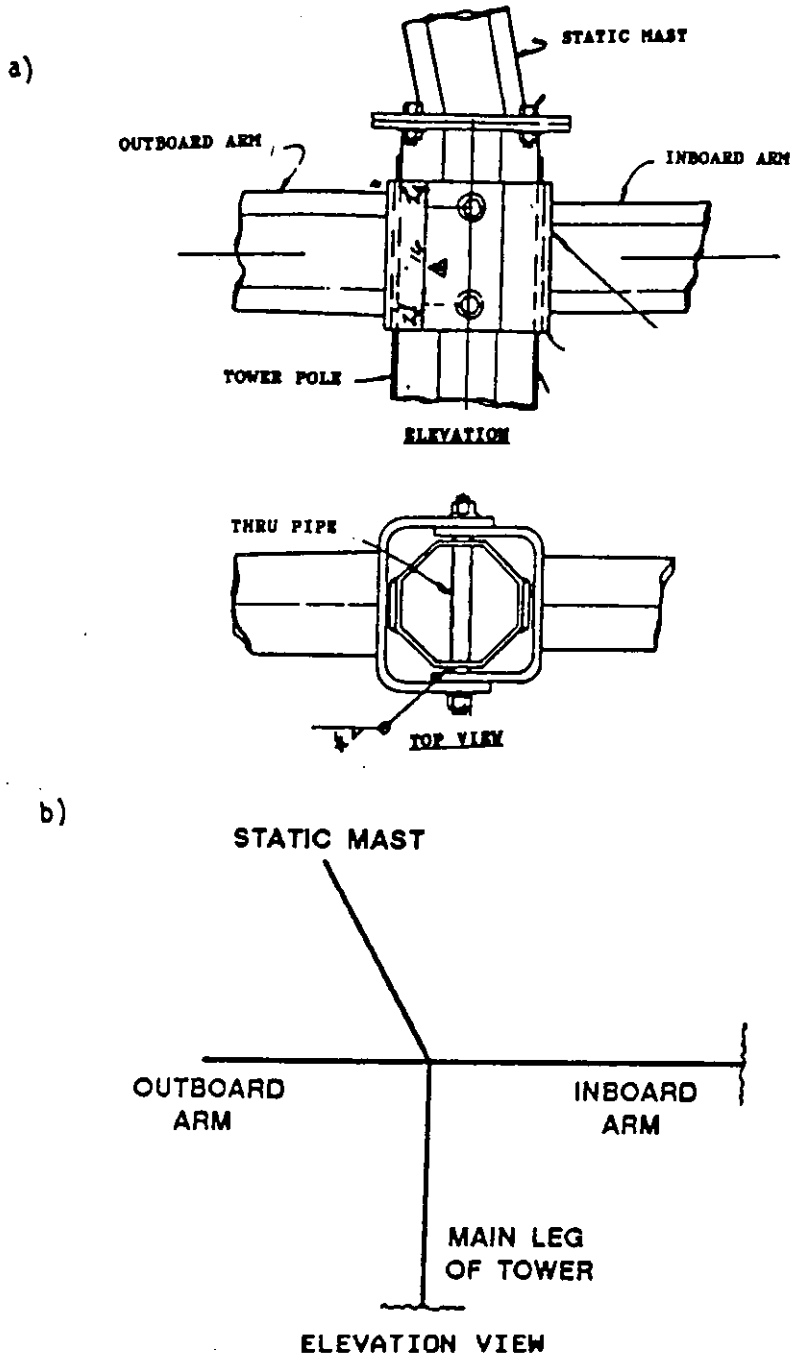

Fig. 4.6: A typical joint of the inboard arm, outboard arm, static mast and tower leg; a) elevation and top view of joint, b) finite element idealization of the joint.

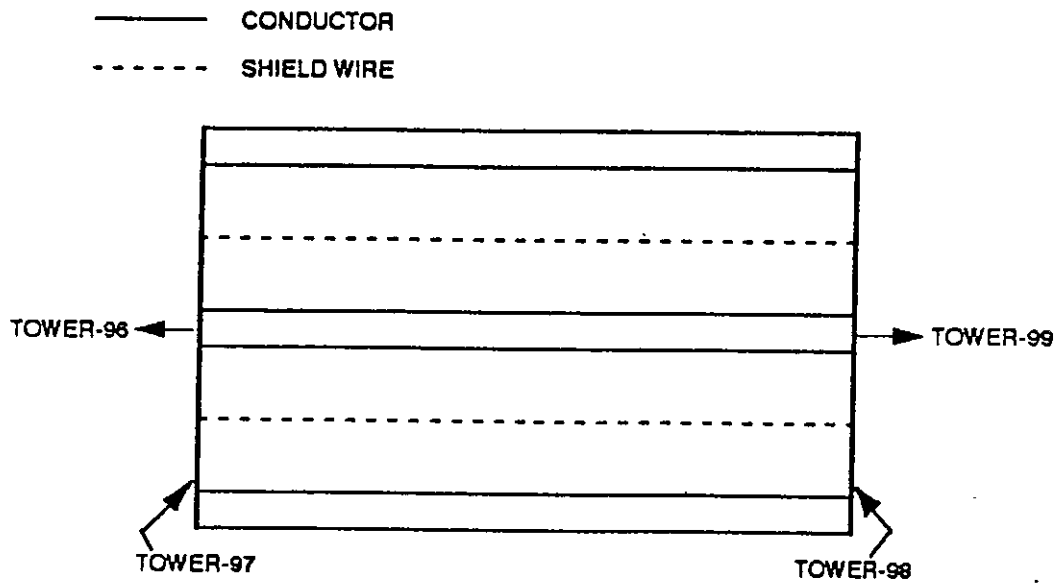

Fig. 4.7: Plan view of a typical span of conductors and shield wires.

a yoke plate as shown in Fig. 4.8. For simplification in modelling the structure, the yoke plates were not included, and the two conducting wires were connected directly to the insulators.

The poles of the structure contained three sections spliced and welded together as shown in Fig. 4.9. In modelling this joint, continuity between these sections was assumed. Structure bracings were assumed to carry only axial loads.

Figure 4.10 shows the location of the nodes within the finite element models for Tower 281 used in both Model 1 and Model 2 with the exception that Model 2 did not include the insulators. The other two structures in Model 1 were identical to Tower 281. The locations of the applied

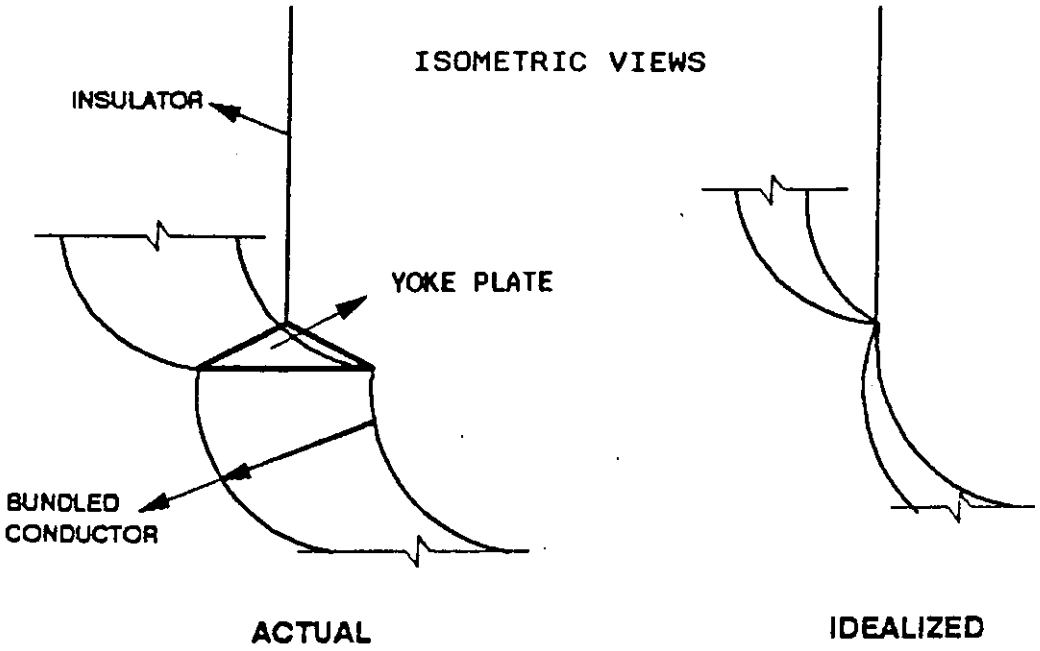

Fig. 4.8: Attachment of the bundled conductor with the structure insulator and its idealization.

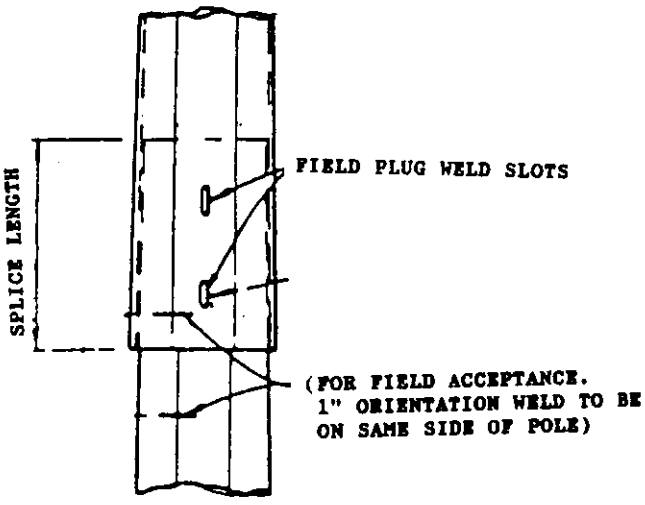

Fig. 4.9: Splicing and welding of the two sections of the main leg.

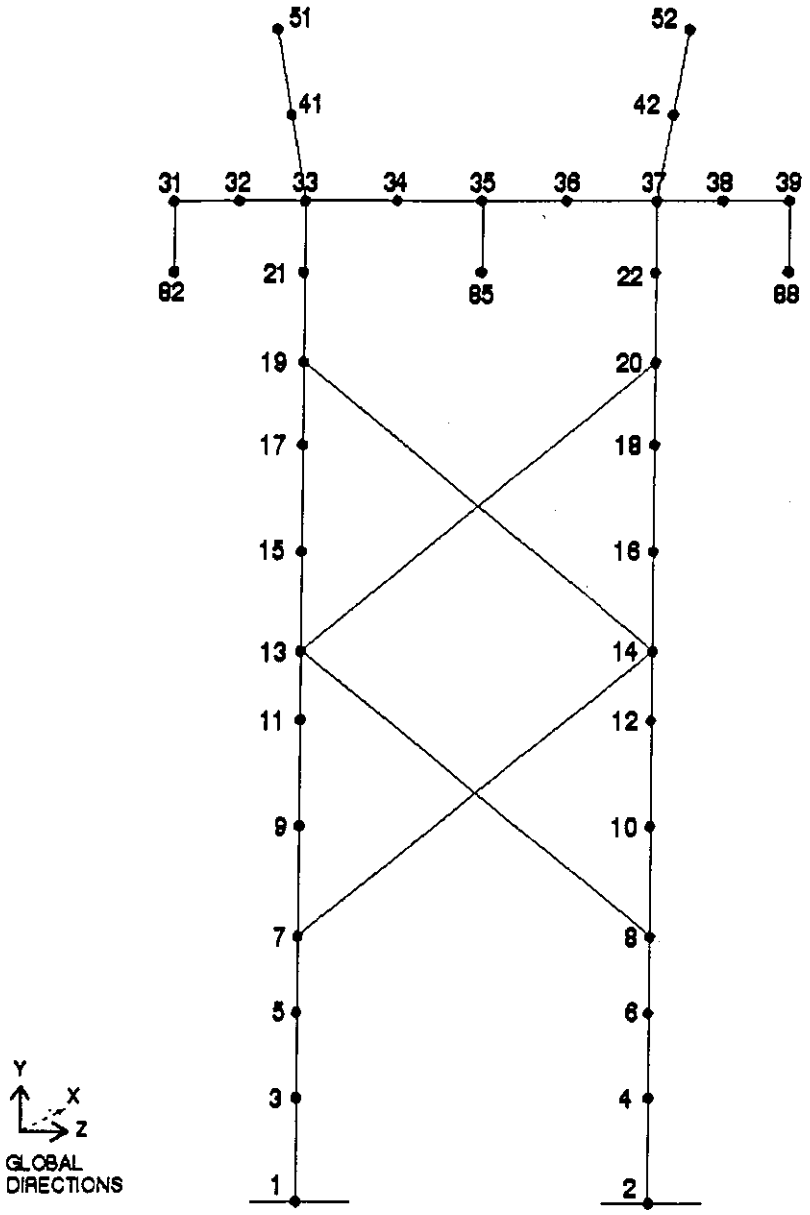

Fig. 4.10: Location of nodes within the finite element models for Tower 281.

forces in Model 2 are shown in Fig. 4.11.

4.2.2 Loads

Overhead electric transmission line structural systems, in general, respond nonlinearly to applied loads. The magnitude of the nonlinearity varies depending on the loads and structural component and type. The transmission structures encountered in this study are classified as steel pole structures which are designed to resist relatively small loads acting in the direction of the conductors from stringing conditions. Therefore, then structures may undergo large deformations under relatively small load imbalances requiring consideration of large deformation in the analysis. This was accomplished in the ETADS program using the available "large displacement" option.

As mentioned previously, elastic material was used in Model 1, and inelastic material behavior was used in Model 2. The non-linear material stress-strain relationship used is a bilinear elastic-plastic relation (see Fig. 4.12). The stress-strain relationship was defined by the elastic and inelastic modulus, E and E_t, respectively. The inelastic modulus, E_t, was assumed to be 0.035% of the elastic modulus, E, to avoid numerical problems associated with the elastic-perfect plastic stress-strain relationship. The value of 0.035% was arbitrarily chosen.

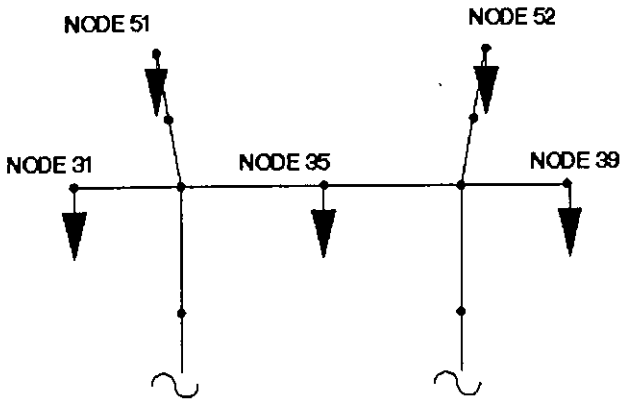

Fig. 4.11: Location of applied forces for finite element model in Model 2.

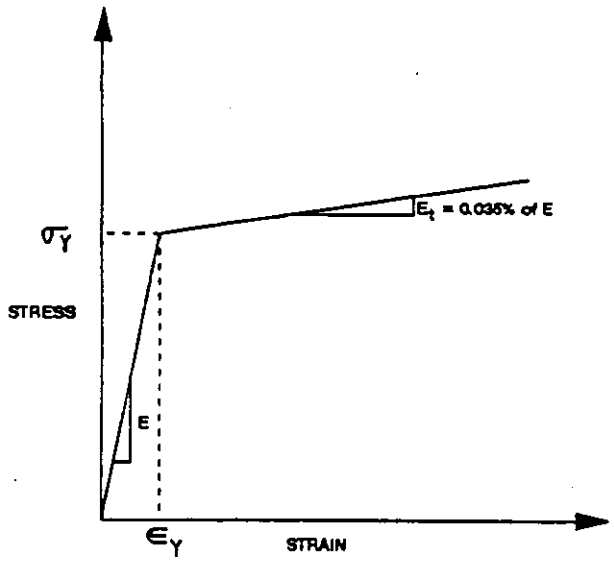

Fig. 4.12: Bilinear elastic-plastic stress-strain relationship used for the structure material.

4.3 Development of the Fragility Curve

The reliability procedure outlined in Chapter 3 was applied to an existing transmission line structure by first analyzing Model 1 under incremental ice loading. This analysis established the relationship between the ice thickness on the conductors and the forces induced at nodes 31, 35, 39, 51, and 52 (see Fig. 4.11). These forces were then used as an input to perform the structural analysis of Model 2. The analysis was continued and all possible failure modes such as buckling, plastic collapse and insulator failure were investigated.

4.3.1 Results of model 1 analysis

Model 1 was loaded in increments of 0.1 in. of ice until 2.0 in. of ice on the conductors was accumulated. The global components of the forces (see Fig. 4.10) at nodes 31, 35, 39, 51 and 52 were recorded. The results of this analysis are shown in Table 4.1.

As would be expected, there is a non-linear relationship between the accumulation of ice and the forces on the structure. Also, the predominate direction of the resulting forces is in the vertical in-plane direction (or Fy) due to the weight of the ice and conductors. These forces, Fy, are negative because of the defined coordinate system shown in Fig. 4.10.

Table 4.1: Forces at nodes 31, 35, 39, 51 and 52 due to various ice thicknesses on the conductors.

ICE THICKNESS (in.)	NODES 31, 35, & 39		NODES 51 & 52	
	$Fy^{(a)}$ (kips)	$Fz^{(b)}$ (kips)	$Fy^{(a)}$ (kips)	$Fz^{(b)}$ (kips)
0.0	-3.19	0.01	-0.35	0.09
0.1	-3.59	0.02	-0.43	0.11
0.2	-4.05	0.03	-0.53	0.13
0.3	-4.58	0.05	-0.67	0.17
0.4	-5.17	0.07	-0.84	0.21
0.5	-5.84	0.09	-1.04	0.25
0.6	-6.56	0.12	-1.28	0.30
0.7	-7.35	0.16	-1.54	0.36
0.8	-8.20	0.21	-1.84	0.43
0.9	-9.12	0.27	-2.17	0.50
1.0	-10.11	0.34	-2.53	0.58
1.1	-11.16	0.43	-2.93	0.65
1.2	-12.27	0.53	-3.35	0.73
1.3	-13.45	0.65	-3.81	0.82
1.4	-14.69	0.79	-4.30	0.91
1.5	-15.99	0.95	-4.83	1.01
1.6	-17.36	1.13	-5.38	1.10
1.7	-18.79	1.34	-5.97	1.19
1.8	-20.28	1.58	-6.60	1.28
1.9	-21.84	1.84	-7.25	1.36
2.0	-23.45	2.14	-7.94	1.45

(a) Vertical in-plane loading
(b) Lateral out-of-plane loading

4.3.2 Buckling failure

The buckling analysis considered only the forces acting vertically assuming that there was no longitudinal direction imbalance forces. This analysis was accomplished using Model 2.

The buckling analysis option was used, and the forces in the vertical in-plane direction corresponding to 2 in. of ice on the conductors was input as applied loads. Classical Eigenbuckling Analysis was used to determine the critical load or loads. Actually, the applied load is arbitrary since the analysis gives a load multiplier to find the critical loads based on the applied loads.

The result of the eigenbuckling analysis was used as the mean value of the variable, x_v, which represents the sum of the vertical forces acting on the structure.

The regression analysis outlined in Chapter 3 was performed using the variables, x_{ice} (which represents ice thickness) and x_v (which represents the sum of the forces in the vertical in-plane direction). These variables were obtained from Table 4.1. For example, when the x_{ice} equals 0.5 in., x_v equals the sum of Fy at nodes 31, 35, 39, 51 and 52 is:

$$x_v = 5.84 + 5.84 + 5.84 + 1.04 + 1.04 = 19.60 \ kips \qquad (4.1)$$

Only the magnitude of the Fy forces is used, so the values for x_v are all positive. The SAS statistical software was

utilized to perform the analysis and to formulate the failure function, $G_B\{x\}$ using the data points which consist of the variables x_{ice} and x_v. This analysis yielded the following failure function:

$$G_B\{x\} = 10.28 + 12.19\,x_{ice} + 12.94\,x_{ice}^2 - x_v \qquad (4.2)$$

4.3.3 Insulator failure

Failure of any of the three insulators can also be induced by a heavy ice accumulation on the conductors. The axial force in the conductors, x_a, i.e., Fy in Table 4.1.

The data points for the regression analysis consisted of the variables, x_{ice} (from the previous failure mode) and x_a. A regression analysis of these data points using SAS was performed and the resulting failure function for the insulator, $G_I\{x\}$, is:

$$G_I\{x\} = 3.05 + 3.66\,x_{ice} + 3.26\,x_{ice}^2 - x_a \qquad (4.3)$$

This equation represents the failure of a single insulator and was used to describe all three failures.

Failure of an insulator does not necessarily constitute failure of the structure, but should be considered as one possible failure mode.

4.3.4 Plastic mechanism failures

4.3.4.1 Plastic mechanism of cross arm

This failure mode deals with the formation of a plastic mechanism that results in a large rotation leading to structural collapse. Previous analysis performed in Refs. 1 and 3 showed that the first plastic hinge will form at the cross arm-pole connection (see Fig. 4.13).

In this work, to simplify this failure mode, a simple cantilever beam was used to study the plastic mechanism of the cross arm. The resulting moments at the end of the cantilever arm are listed in Table 4.2 for various ice thicknesses.

The regression analysis resulted in the following failure function of the cross arm:

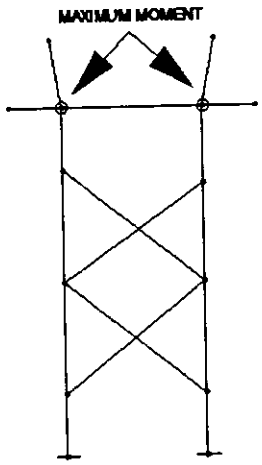

Fig. 4.13: Location of maximum moment on the transmission line structure.

Table 4.2: Moments at location between the cross-arm and pole.

ICE THICKNESS (in.)	MOMENT (in*kip)	ICE THICKNESS (in.)	MOMENT (in*kip)
0.0	789.48	1.0	2325.19
0.1	878.28	1.1	2558.09
0.2	980.39	1.2	2804.25
0.3	1098.04	1.3	3065.88
0.4	1229.00	1.4	3340.75
0.5	1377.70	1.5	3628.82
0.6	1537.50	1.6	3932.22
0.7	1712.82	1.7	4248.11
0.8	1901.43	1.8	4572.23
0.9	2105.56		

$$G_p\{x\} = 790.55 + 798.62\,x_{ice} + 751.55\,x_{ice}^2 - 15.07\,x_{ice}^3 - x_m \qquad (4.4)$$

where,

$G_p\{x\}$= failure equation for the formation of plastic hinge,

x_m = the moment at the connection between the structure arm and leg.

This limit state equation applies for both left and right sides of the transmission line structure assuming symmetry. Therefore, this failure type includes two individual failure modes, one for the right arm and one for the left arm.

As with the insulator failures, the failure of the cross arm does not imply failure of the entire structure. However, one must consider this mode when investigating the failure of the transmission line structure.

4.3.4.2 Plastic collapse of pole

Plastic collapse of the pole may occur when an insulator or an outboard arm of an adjacent structure fails resulting in a large imbalance force. This imbalance situation may also occur when a conductor is broken which as illustrated in Fig. 4.14. The figure depicts a broken middle conductor between Tower "B" and Tower "C". Such an occurrence is important to investigate because the resulting imbalance force may yield a domino pattern of failure.

To investigate this case, Model 2 was analyzed considering vertical in-plane forces at nodes 31, 35, and 39. The sum of these forces is referred to hereafter as V. A horizontal out-of-plane force, H, at node 35 representing an imbalance force was added to the model. The analysis was performed four times considering various levels of interaction between the vertical and horizontal forces. The levels of interaction between the forces V and H are listed below:

- H = 0.0 V
- H = 0.2 V
- H = 0.4 V
- H = 0.6 V
- H = 0.8 V

The first interaction was studied in Section 4.3.2 when investigating the buckling failure of the structure.

In the structural analysis, these forces were incremented following the guidelines of the limit analysis procedure in ETADS, while the induced moments in the poles were monitored.

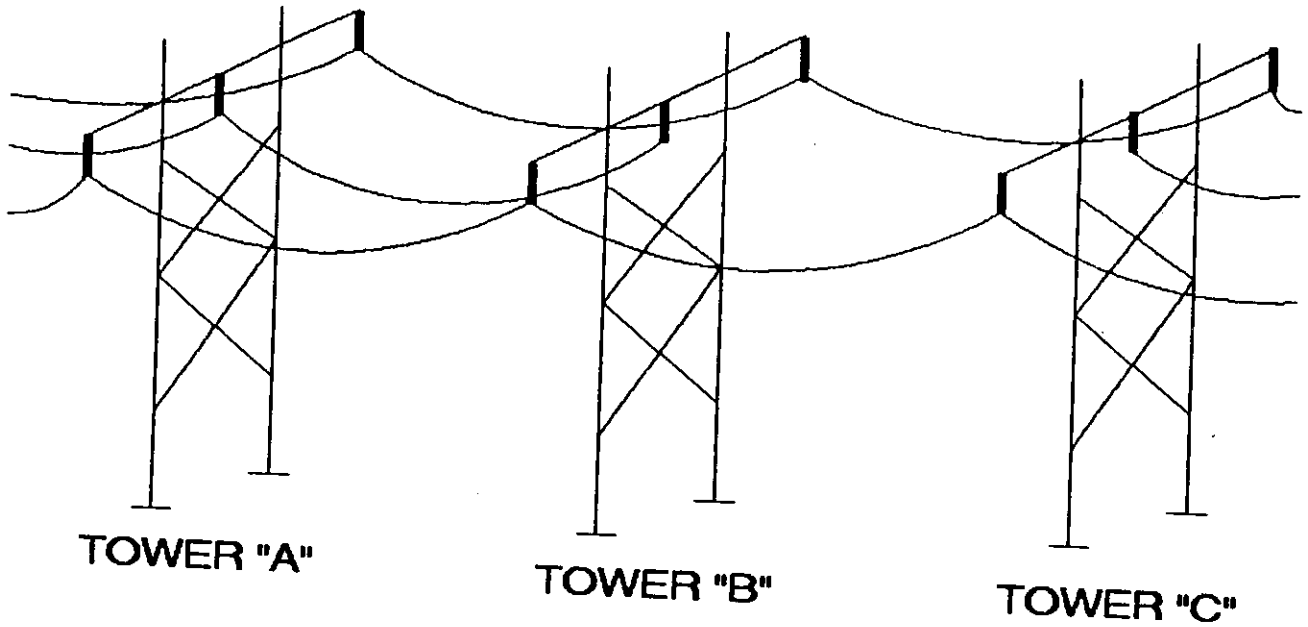

Fig. 4.14: Force imbalance created at Tower "A" and Tower "C" due to a broken conductor between Tower "B" and Tower "C".

Since the pole is a tapered member, the locations of yielding was indeterminate and is not at the base of the pole as one may expect. When full plastic hinges form at these locations, an unrestricted rotation under any additional load will occur leading to an unstable structure indicating the loss of the structure integrity.

Due to symmetry, the formation of a plastic hinge on one pole of the transmission line corresponds to the formation of a plastic hinge in the other pole. The failure equations were developed for plastic collapse of five pairs of nodes (see Fig. 4.10), and those pairs are:

- nodes 1 and 2
- nodes 3 and 4
- nodes 5 and 6
- nodes 7 and 8
- nodes 9 and 10

For convenience, reference to these pairs of nodes will only include the number of the first node listed.

For interaction level H/V=0.2, the following failure equations were developed based on the moments obtained from the structural analyses:

$$G_1^{0.2}\{x\} = -75.08 - 26.99\,V - 0.206\,x_1 * H + x_1 \qquad (4.5)$$

$$G_3^{0.2}\{x\} = -62.99 - 25.95\,V - 0.208\,x_3 * H + x_3 \qquad (4.6)$$

$$G_5^{0.2}\{x\} = -51.43 - 24.86\,V - 0.208\,x_5 * H + x_5 \qquad (4.7)$$

$$G_7^{0.2}\{x\} = -33.33 - 22.73\,V - 0.213\,x_7 * H + x_7 \quad (4.8)$$

$$G_9^{0.2}\{x\} = -18.63 - 20.76\,V - 0.216\,x_9 * H + x_9 \quad (4.9)$$

where,

$G_1^{0.2}\{x\}$ represents the failure mode that occurs at nodes 1 and 2 for interaction level H/V=0.2

$G_3^{0.2}\{x\}$ represents the failure mode that occurs at nodes 3 and 4 for interaction level H/V=0.2

$G_5^{0.2}\{x\}$ represents the failure mode that occurs at nodes 5 and 6 for interaction level H/V=0.2

$G_7^{0.2}\{x\}$ represents the failure mode that occurs at nodes 7 and 8 for interaction level H/V=0.2

$G_9^{0.2}\{x\}$ represents the failure mode that occurs at nodes 9 and 10 for interaction level H/V=0.2

x_1 = the moment at nodes 1 and 2

x_3 = the moment at nodes 3 and 4

x_5 = the moment at nodes 5 and 6

x_7 = the moment at nodes 7 and 8

x_9 = the moment at nodes 9 and 10

Similarly, the failure equations were developed for interaction level H/V=0.4 based on the moments obtained from the structural analyses:

$$G_1^{0.4}\{x\} = -554.36 - 199.55\,H^2 + x_1 \quad (4.10)$$

$$G_3^{0.4}\{x\} = -504.19 - 193.61\,H^2 + x_3 \quad (4.11)$$

$$G_5^{0.4}\{x\} = -455.28 - 187.07\,H^2 + x_5 \quad (4.12)$$

$$G_7^{0.4}\{x\} = -347.67 - 173.19\,H^2 + x_7 \quad (4.13)$$

$$G_9^{0.4}\{x\} = -306.44 - 159.90\,H^2 + x_9 \quad (4.14)$$

where,

$G_1^{0.4}\{x\}$ represents the failure mode that occurs at nodes 1 and 2 for interaction level H/V=0.4

$G_3^{0.4}\{x\}$ represents the failure mode that occurs at nodes 3 and 4 for interaction level H/V=0.4

$G_5^{0.4}\{x\}$ represents the failure mode that occurs at nodes 5 and 6 for interaction level H/V=0.4

$G_7^{0.4}\{x\}$ represents the failure mode that occurs at nodes 7 and 8 for interaction level H/V=0.4

$G_9^{0.4}\{x\}$ represents the failure mode that occurs at nodes 9 and 10 for interaction level H/V=0.4

For interaction level H/V=0.6, the failure equations were developed and are listed below:

$$G_1^{0.6}\{x\} = -791.58 - 137.00H^2 + x_1 \quad \textbf{(4.15)}$$

$$G_3^{0.6}\{x\} = -727.63 - 132.39H^2 + x_3 \quad \textbf{(4.16)}$$

$$G_5^{0.6}\{x\} = -664.72 - 127.43H^2 + x_5 \quad \textbf{(4.17)}$$

$$G_7^{0.6}\{x\} = -560.40 - 117.14H^2 + x_7 \quad \textbf{(4.18)}$$

$$G_9^{0.6}\{x\} = -471.08 - 107.45H^2 + x_9 \quad \textbf{(4.19)}$$

where,

$G_1^{0.6}\{x\}$ represents the failure mode that occurs at nodes 1 and 2 for interaction level H/V=0.6

$G_3^{0.6}\{x\}$ represents the failure mode that occurs at nodes 3 and 4 for interaction level H/V=0.6

$G_5^{0.6}\{x\}$ represents the failure mode that occurs at nodes 5 and 6 for interaction level H/V=0.6

$G_7^{0.6}\{x\}$ represents the failure mode that occurs at nodes 7 and 8 for interaction level H/V=0.6

$G_9^{0.6}\{x\}$ represents the failure mode that occurs at nodes 9 and 10 for interaction level H/V=0.6

Lastly, the failure equations for interaction level H/V=0.8 were developed and are listed below:

$$G_1^{0.8}\{x\} = -1025.35 - 105.05H^2 + x_1 \quad \textbf{(4.20)}$$

$$G_3^{0.8}\{x\} = -951.63 - 101.04H^2 + x_3 \quad \textbf{(4.21)}$$

$$G_5^{0.8}\{x\} = -878.61 - 96.81H^2 + x_5 \qquad (4.22)$$

$$G_7^{0.8}\{x\} = -754.79 - 88.32H^2 + x_7 \qquad (4.23)$$

$$G_9^{0.8}\{x\} = -647.73 - 80.44H^2 + x_9 \qquad (4.24)$$

where,

$G_1^{0.8}\{x\}$ represents the failure mode that occurs at nodes 1 and 2 for interaction level H/V=0.8

$G_3^{0.8}\{x\}$ represents the failure mode that occurs at nodes 3 and 4 for interaction level H/V=0.8

$G_5^{0.8}\{x\}$ represents the failure mode that occurs at nodes 5 and 6 for interaction level H/V=0.8

$G_7^{0.8}\{x\}$ represents the failure mode that occurs at nodes 7 and 8 for interaction level H/V=0.8

$G_9^{0.8}\{x\}$ represents the failure mode that occurs at nodes 9 and 10 for interaction level H/V=0.8

4.3.5 Combination of failure modes

The analysis outlined above showed that there are six failure modes for the undamaged transmission line structure, (1) failure under vertical load that causes buckling of the transmission pole; (2) three failure modes that are associated with the three insulators; and (3) two failure modes that results from formation of plastic hinges on the right and left of the cross arm connection. Equations (4.2)-(4.4) represent the failure functions of these listed modes.

The remaining failure equations, Eqs. (4.5)-(4.24), are developed based on the broken conductor scenario, and are considered separately. This assumption was made because these last equations are based on different conditions than the first set of failure equations.

All of the failure functions used the Lind-Hasofer method (see Section 3.2.2) to predict the failure probabilities associated with each modes. Only the first set of failure functions, Eqs. (4.2)-(4.4), were combined to form upper and lower bounds on the probability of structural failure using the method in Section 3.3.

Regardless of the equation, the reliability calculations require the definition of the mean and coefficient of variation of the variables used in the failure functions. All of the variables in this example have an assumed normal distribution, and the mean and coefficient of variation of these variables are listed in Table 4.3.

A spreadsheet with the Lind-Hasofer equations integrated, was utilized to calculate the reliability index, ß, that corresponds to different ice thicknesses. This spreadsheet is similar to the one described in Section 3.4.1. The probability of failure was then calculated using the standard normal probability tables. Figure 4.15 shows the probability of failure for the failure modes corresponding to the undamaged transmission line structure.

The probability of failure of these modes were combined following the procedure outlined in Section 3.3. The upper and lower limits for the structure failure probability excluding a broken conductor case is shown in Fig. 4.16.

For the remaining failure functions given in Eqs. (4.5)-

Table 4.3: Variables with mean values and coefficient of variation (COV).

Variable	Mean	COV
x_{ice}	(variable)	0.10
H	(variable)	0.10
x_v	80 kips	0.05
x_a	18 kips	0.05
x_m	4,578 in*kips	0.05
x_1	10,618 in*kips	0.05
x_3	10,106 in*kips	0.05
x_5	7,025 in*kips	0.05
x_7	6,337 in*kips	0.05
x_9	5,735 in*kips	0.05

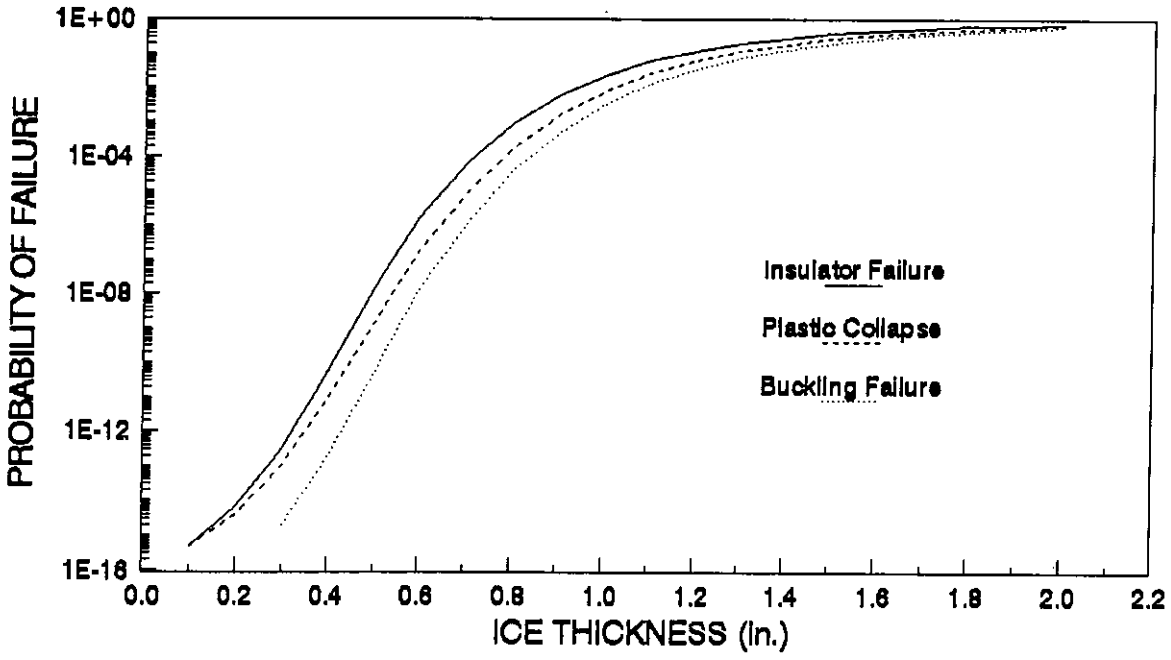

Fig. 4.15: Probability of failure curves for individual failure modes for undamaged transmission line structure.

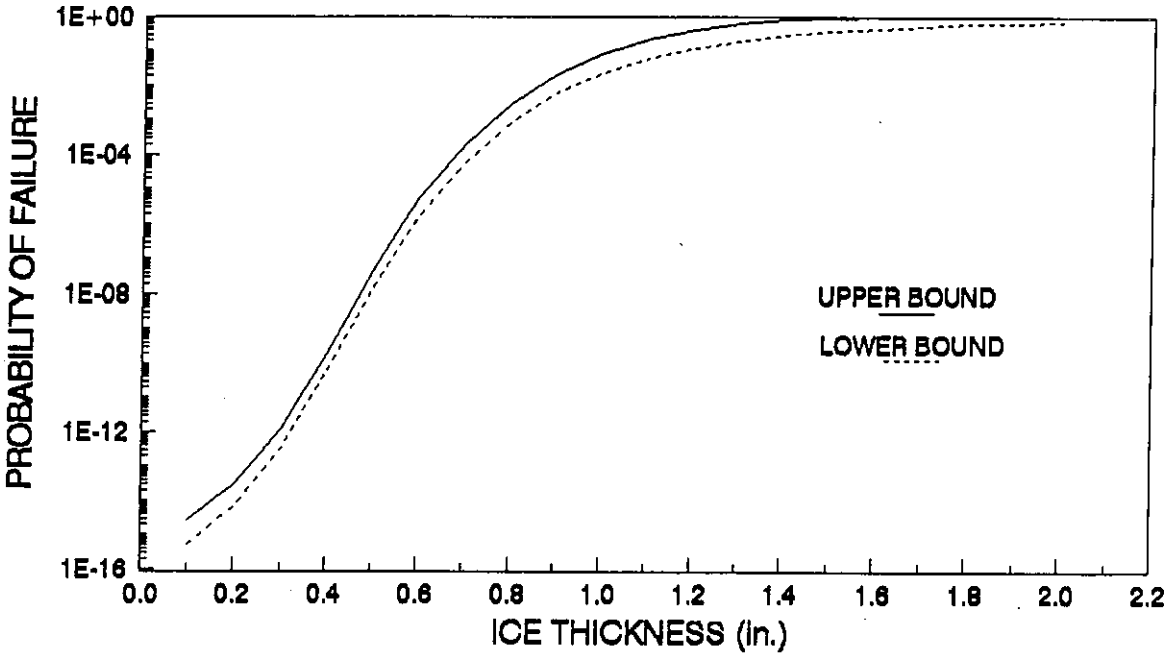

Fig. 4.16: Fragility curve with upper and lower bounds for undamaged transmission line structure.

(4.24), the same procedure was followed except that no combination of the failure probabilities was considered. Since these equations do not pertain to the same loading conditions, these equations cannot be combined to form an overall structural probability of failure. However, the probability of failure for the individual failure modes were found. Figure 4.17 shows the five probability of failure curves for interaction level, H/V=0.20, and Fig. 4.18 shows those probability of failure curves for interaction level, H/V=0.4. Figures 4.19 and 4.20 display the probability of failure curves for interaction levels, H/V=0.6 and H/V=0.8 respectively. Figure 4.21 depicts the dominate failure mode

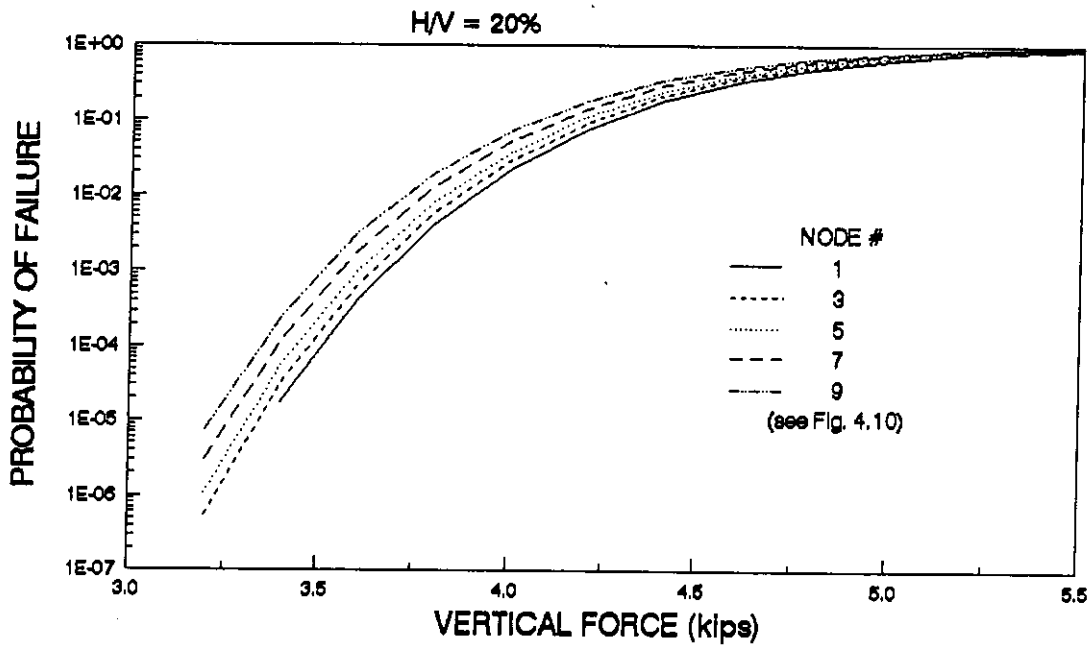

Fig. 4.17: Probability of failure curves for individual failure modes for broken insulator case where the interaction level is H/V=0.2.

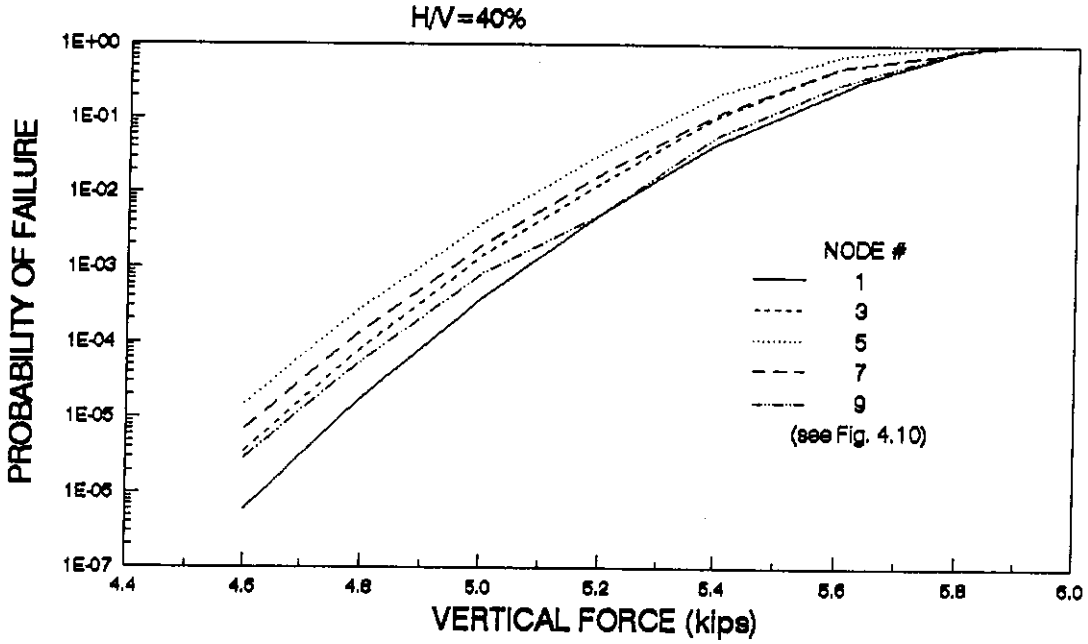

Fig. 4.18: Probability of failure curves for individual failure modes for broken insulator case where the interaction level is H/V=0.4.

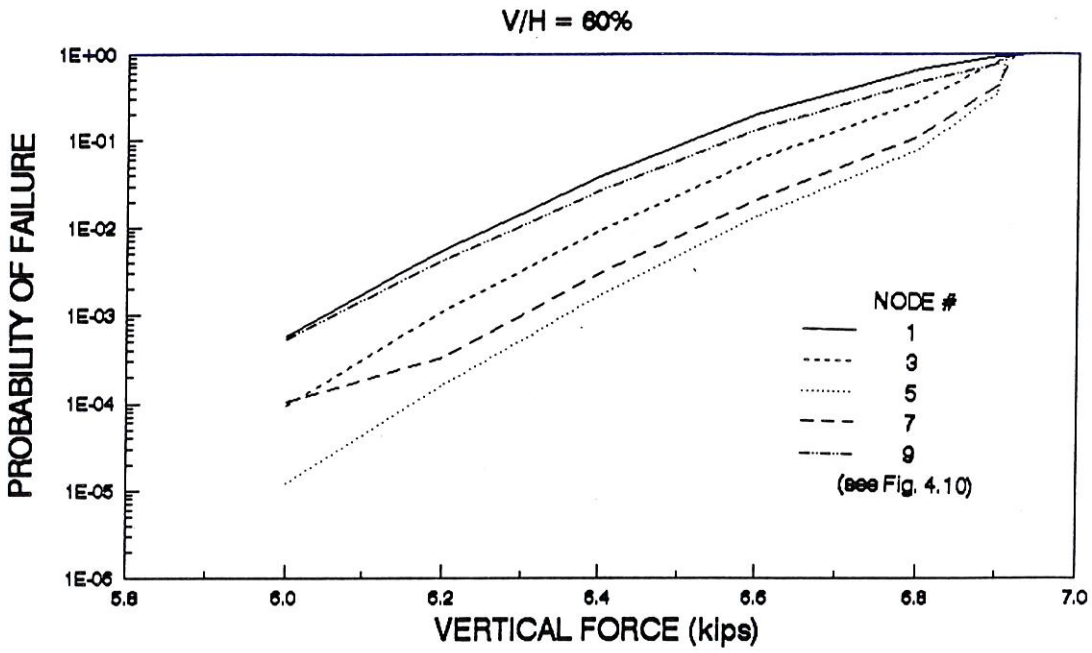

Fig. 4.19: Probability of failure curves for individual failure modes for broken insulator case where the interaction level is H/V=0.6.

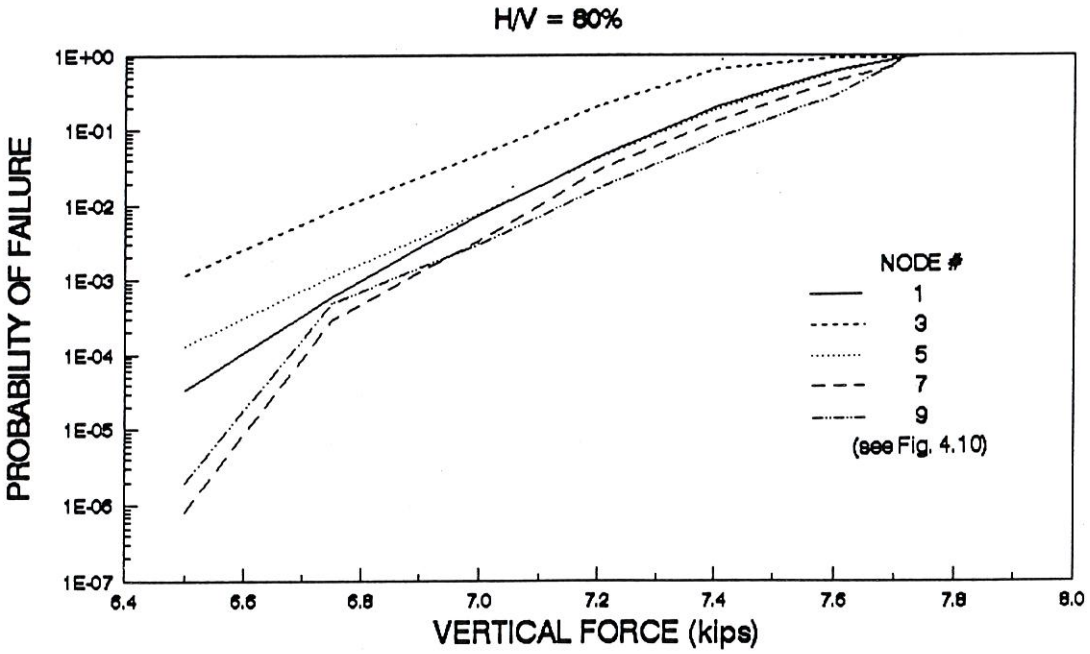

Fig. 4.20: Probability of failure curves for individual failure modes for broken insulator case where the interaction level is H/V=0.8.

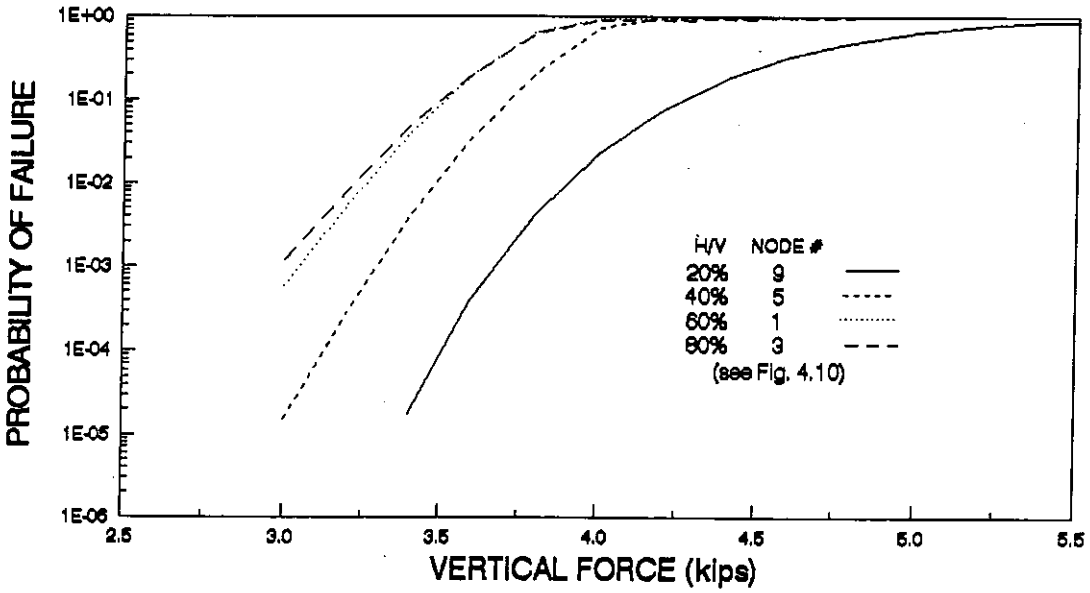

Fig. 4.21: Probability of failure curves for the dominate failure modes of the four interaction levels.

of each interaction level which are:

1. For interaction level, H/V=0.2, the plastic collapse of nodes 9 and 10.

2. For interaction level, H/V=0.4, the plastic collapse of nodes 5 and 6.

3. For interaction level, H/V=0.6, the plastic collapse of nodes 1 and 2.

4. For interaction level, H/V=0.8, the plastic collapse of nodes 3 and 4.

4.3.6 Interpretation of fragility curves

The fragility curve for the undamaged transmission line structure, shown in Fig. 4.16, represents the probability of failure for a given ice thickness. The ice storms in Mid-Iowa, which resulted in the previous studies, produced an approximate ice thickness of 1.25 to 1.5 in. of ice

accumulation on the conductors. For 1.25 in. of ice, the probability of structural failure is 15%-45% based on the calculations made in this study. For 1.5 in. of ice, the probability increases to the range of 35%-85%. In this case, failure most likely will result from buckling of the line. This is true if and only if no broken insulator or conductor occurs.

The probabilities of failure for the ice thicknesses of 1.25 in. and 1.5 in. indicate that there is high chance that the transmission line structure would be structural damaged during an ice storm which produced this amount of ice. Based on this information, one might say that the structure needs to be strengthened. But if the ice storm only occurs once every 50-years, then strengthening this structure may not be an economically wise decision. The fact that two of these ice storms occurred in Iowa within a span of 18 months does not indicate that these storms are typical of this area. There is a trade-off between the goal to prevent any failure and the cost of such a venture.

Alternatively, Fig. 4.21 can be used to interpret the probability of failure for a given ice thickness; however, the probability of failure is not interpreted the same as the previous case. The resulting probability is the failure probability of a damaged transmission line structure, such as one with a broken conductor or insulator.

To exemplify this case, consider an ice thickness of 0.5 in. The sum of the vertical forces is 19.6 kips (see Table 4.1). Assuming an interaction level between the horizontal force and the vertical force as H/V=0.2, the horizontal force is 3.9 kips. This corresponds to a probability of failure of approximately 5.0%. But the chance of the transmission line structure having a broken conductor at 0.5 in. of ice is negligible.

If the ice thickness was 1.25 in., which has a significant probability of the structure resulting in a broken conductor, the sum of the vertical forces is 46.0 kips. Again assuming the same interaction level (H/V=0.2), the horizontal force is 9.2 kips. Based on the calculations in this work, this force corresponds to a probability of failure of almost 100%. Realistically, this means that once the ice loads results in breaking a conductor, the probability of structural failure would be significant.

Engineering economic analysis using these probability of failure curves, Fig. 4.16 and Fig. 4.21, would provide engineers with more data with which to evaluate the condition of the transmission line structure under consideration. An engineering economic analysis may be accomplished using methods described in Ref. 23.

5. SUMMARY AND CONCLUSIONS

5.1 Summary

The occurrence of two major ice storms in Mid-Iowa resulted in the damage and collapse of many transmission line structures. The first happened on March 7, 1990 and caused 68 failed structures. On October 31, 1991, the second storm hit Iowa and caused the most destruction in Iowa's history. These events were previously investigated and analyzed by others to determine possible failure scenarios. The first ice storm analysis suggested that a probabilistic analysis needed to be performed.

The design of transmission line structures typically does not encompass probabilistic theory or reliability concepts such as Load and Resistance Factor Design (LRFD) that has been recently adopted in design of steel buildings. However, some reliability based design methods for transmission lines have been developed; two methods were proposed by the American Society of Civil Engineers and International Electrotechnical Commission. As designers use these procedures, the acceptance of reliability based design for transmission line structures should continue to grow.

Meanwhile, the methods followed to perform a probabilistic analysis of existing transmission line structures are varied. The development of the required limit state functions for these procedures require knowledge of

closed form solutions which involves rigorous manipulations of equations for a transmission line structure. The reliability analysis procedure developed in this study does not require this knowledge.

The limit state function needed to perform a reliability analysis was developed herein using a regression analysis. Once the limit state function was established, the Lind-Hasofer FOSM method was used to analyze the limit state function and to estimate the probability of failure associated with the various failure modes and corresponds to different load levels. These probabilities were then used to construct fragility curves for the system failure probability.

In this study, the load was the accumulation of ice on the conductors and shield wires. Four basic types of failures of the transmission line structure were investigated:

- buckling of the structure poles,
- failure of the insulators, and
- formation of a plastic hinge at the connection point between the outboard arm and pole.
- failure of the transmission line structure subjected to unbalanced forces due to a broken conductor buckling of the structure poles.

Specifically, the last type of failure of the transmission line structure dealt with a broken central conductor. This condition resulted in the formation of plastic hinges in the poles of the transmission line structure.

5.2 Conclusions

The resulting fragility curves provide information about the existing transmission line structure. This information can be use to determine the condition of a structure under different loadings. The condition of a structure is interpreted by the probability of failure.

The probability of structural failure was determined for an ice thickness on the conductors of 1.5 in. to be between 35% and 85%. After the ice storm in Mid-Iowa on March 7, 1990, the amount of ice on the conductors was recorded as 1.25-1.50 in. The analysis of the transmission line involved in this ice storm determined that critical load of the structure happened when the ice thickness was between 1.50 and 1.75 in. of ice [1]. Based on this information, one might say that the structure needs to be strengthened. But if the ice storm only occurs once every 50-years, then strengthening this structure may not be an economically wise decision. Interpretation of the probability of failure data should be compared with the frequency of the loading in order to make judgements about the condition of a structure. There is a trade-off between the goal to prevent any failure and the cost of such a venture.

5.3 Recommendations for Further Research

The probabilistic analysis procedure presented in this study may be further investigated to include different

applications, more variables, the variability of more parameters and the uncertainty of the variables.

Many other scenarios may be considered using this probabilistic analysis procedure, including different loading conditions, combinations of various loading conditions, and different types of transmission line structures. Various climatic conditions such as wind and the combination of wind and ice accumulation are possible scenarios.

Some variables to incorporate into the analysis are the difference of adjacent span lengths between transmission line structures and the angle between structures.

The parameters which were included in this work are ice thickness, plastic moment capacities of joints in the structure, and strength of the insulators. These parameters could be separated so that the geometric dimensions of the structure and material properties associated with the parameters could be included in the analysis. The inclusion of the geometric dimensions and material properties would increase the computations and structural analysis runs significantly, but the benefit would be the inclusion of the variability of these parameters in the analysis. Sensitivity studies would indicate which parameters have the most effect on the probability of failure.

REFERENCES

1. S. Gupta. "Nonlinear Analysis of Transmission Line Structures Subjected to Ice Loads." Thesis, Iowa State U, 1991.

2. "Electric Power Research Institute's TLWorkstation software, module ETADS." Palo Alto, CA, July 1990.

3. A. Nafie. "Failure Analysis of Transmission Line Structures." Thesis, Iowa State U, 1993.

4. H. J. Hillarker. "Preliminary monthly weather summary - November 1991." State Climatologist's report, Iowa Department of Agriculture and Land Stewardship, Des Moines, IA.

5. Y. Ibrahim. "General Strategy for Structural Systems Reliability Analysis." *Journal of Structural Engineering* vol. 114 (March 1991): 789-807.

6. H. O. Madsen, S. Krenk and N.C. Lind. *Methods of Structural Safety*. Englewood Cliffs, NJ: Prentice-Hall, 1986.

7. L. Griemann and W. Knapp. *Reliability Assessment for the Buckling of Stiffened Cylinders*. Final Report submitted to Conoco, Inc.,ISU-ERI-Ames-83284, ERI Project-1564. Engineering Research Institute, Iowa State U, June 1983.

8. P. Thoft-Christensen and Y. Murotsu. *Application of Structural Systems Reliability Theory*. Berlin, Heidelberg: Springer-Verlag, 1986.

9. SAS Institute Inc. *SAS User's Guide: Statistics, Version 5 Edition*. Cary, NC: SAS Institute Inc., 1985.

10. *National Electrical Safety Code*. National Bureau of Standards. Washington, DC: U.S. Govt. Print. Off., 1989.

11. A. Peyrot, M. Maamouri, H. Dagher and S. Kulendran. "Reliability-Based Design of Transmission Lines: A Comparison of the ASCE and IEC methods." *Third International Conference on Probabilistic Methods Applied to Electric Power Systems*. London: Institute of Electrical Engineering, 1991.

12. *ASCE Guidelines for Transmission Line Structural Loading*. New York, NY: American Society of Civil Engineers, 1991.

13. IEC Technical Committee No. 11, *Loading and Strength of Overhead Transmission Lines*, 1988 draft, International Electrotechnical Commission, Geneva, Switzerland.

14. F. G. Picciano. "The NESC, Probability, Reliability and the Future." *Probabilistic Methods Applied to Electric Power Systems*, Proceeding of the First International Symposium, Toronto, Canada. 11-13 July, 1986. New York, NY: Pergamon Press, 1987.

15. H. J. Dagher, S. Kulendran, A. H. Peyrot and M. Maamouri. "System Reliability Concepts in the Design of Transmission Lines." National Science Foundation MSM-8821079, EPRI-RP1352-11. Final Report, 1992.

16. A. Kamarudin. "A Censoring Technique in the Monte Carlo Simulation Method Applied to Probability Based Distribution Line Wood Pole Design." *Probabilistic Methods Applied to Electric Power Systems*, Proceeding of the First International Symposium, Toronto, Canada. 11-13 July, 1986. New York, NY: Pergamon Press, 1987.

17. A. K. Haldar. "Structural Reliability Analysis of a Transmission Tower using Probabilistic Finite Element Method." *Probabilistic Methods Applied to Electric Power Systems*, Proceeding of the First International Symposium, Toronto, Canada. 11-13 July, 1986. New York, NY: Pergamon Press, 1987.

18. Y. Murotsu, H. Okada, S. Matsuzaki and S. Nakamura. "On the Probabilistic Collapse Analysis of Transmission Line Structures." *Probabilistic Methods Applied to Electric Power Systems*, Proceeding of the First International Symposium, Toronto, Canada. 11-13 July, 1986. New York, NY: Pergamon Press, 1987.

19. A. Haldar. "Recent Failure of a Transmission Line due to Ice in Newfoundland." Fifth International Workshop on Atmospheric Icing of Structures. Tokyo, Japan: Arcadia Ichigaya, 1990.

20. "Tables of the Bivariate Normal Distribution Function and Related Functions." U.S. Department of Commerce, National Bureau of Standards, Applied Mathematics Series, 50. Washington, DC: U.S. Govt. Print. Off., 1953.

21. T. A. Ryan. *Minitab Reference Manual*. Ames, Iowa: Computation Center, Iowa State U, 1981.

22. M. Gorman and F. Moses. "Direct Estimate of Structural

System Reliability," *Seventh Conference on Electronic Computation*. New York, NY: American Society of Civil Engineering, 1979.

23. S. K. Adams. *Engineering Economic Analysis*. New York, NY: McGraw-Hill, 1991.

ACKNOWLEDGEMENTS

I would like to thank my co-major professors, Dr. Fouad Fanous and Dr. Terry Wipf, for all of their support and guidance in my research. Fouad Fanous was especially understanding and helpful.

Most of all, I extend my deepest thanks to my husband, Bob, for everything that he has done to make it possible for me to complete my research.